FTSJ3 is an RNA 2'-O-methyltransferase recruited by HIV to avoid innate immune sensing

Mathieu Ringeard, Virginie Marchand, Etienne Decroly, Yuri Motorin, Yamina Bennasser

FTSJ3 is an RNA 2'-O-methyltransferase recruited by HIV to avoid innate immune sensing

Mathieu Ringeard[1], Virginie Marchand[2], Etienne Decroly[3], Yuri Motorin[4] and Yamina Bennasser[1]

[1] Institut de Génétique Humaine, Laboratoire de Virologie Moléculaire, UMR9002, CNRS, Université de Montpellier, Montpellier, France.

[2] Next-Generation Sequencing Core Facility, UMS2008 IBSLor CNRS-University of Lorraine-INSERM, BioPole, 9 avenue de la Foret de Haye, 54505 Vandoeuvre-les-Nancy, France.

[3] AFMB, CNRS, Aix-Marseille Université, UMR 7257, Case 925, 163 Avenue de Luminy, 13288 Marseille Cedex 09, France.

[4] IMoPA UMR7365 CNRS-University of Lorraine, BioPole, 9 avenue de la Foret de Haye, 54505 Vandoeuvre-les-Nancy, France.

Corresponding author: yamina.bennasser@igh.cnrs.fr

In mammals, RNA 2'-O-methylation is a molecular signature for the discrimination of endogenous from exogenous mRNA by the cellular innate immune system[1-3]. Here we purified TRBP and its interacting partners to identify a DICER-independent TRBP complex containing FTSJ3, a putative 2'-O-methyltransferase (2'O-MTase). In vitro and ex-vivo experiments show that FTSJ3 is a 2'O-MTase that is recruited to HIV RNA through TRBP. Using RiboMethSeq analysis[4], we identified 2'-O-methylated residues on viral genome, and found that FTSJ3 modifies HIV RNA at specific sites. HIV-1 viruses produced in FTSJ3 knock-down cells show reduced 2'-O-methylation and trigger type 1-interferons (IFN) expression in human dendritic cells through the RNA sensor MDA5. This IFN-α and IFN-β induction leads to a reduced HIV expression. Altogether, our study revealed an unexpected mechanism used by HIV to evade innate immune recognition involving the recruitment of TRBP/FTSJ3 complex to viral RNA and its 2'-O-methylation.

Among post-transcriptional modifications of RNA, called epitranscriptome, 2'-O-methylation is present at the 5'-extremity of all mRNAs in mammals and internally at specific residues of tRNA, rRNA, snRNA and cellular mRNA[5,6]. Known for decades for its role in RNA stabilization, its key function in innate immunity has been uncovered recently[1,2]. Cellular mRNAs are capped with a 7-methyl-guanosine (^{m7}G), a 5'-modification crucial for mRNA splicing, export to the cytoplasm, and efficient translation into proteins[7]. In addition, mRNAs in higher Eucaryotes acquire a second modification: a 2'-O-ribose methylation on the first (cap1) and the second transcribed nucleotide (cap2). This modification provides a molecular signature for discrimination of self from non-self mRNA. In the cell, cytoplasmic sensors, such as MDA5 and RIG-I, recognize exogenous unmodified RNAs and activate type-1 interferon production to establish an antiviral state[8,9]. To evade innate immune response, some viruses, including Flaviviruses, encode for their own viral 2'O-MTase that can add a cap1/2 on viral transcripts[10] and in the case of West Nile, Dengue and Ebola viruses can also methylate internal adenosine residues of viral genome in vitro[11,12]. In addition, in other pathogens, such as E.coli strains, tRNA 2'-O-methylation also plays an important role in immunostimulation of human dendritic cells since the loss of unique Gm18 residue in mutant *TrmH* E.coli strain abolishes immunosuppression[13,14]. This is due to the G18 residue of $tRNA^{Tyr}$ that has to be 2'-O-methylated to avoid innate sensing in human cells. In contrast to Flaviviruses, HIV does not encode a 2'O-MTase. However, FTSJ3, a putative host 2'O-MTase, was purified as a partner of TAR RNA binding protein (TRBP), a dsRNA binding

protein known to interact with 5'-RNA leader sequence TAR and facilitate HIV expression[15,16]. Owing to its interaction with TRBP, this putative 2'O-MTase might be recruited to HIV viral genome. FTSJ3 was identified in a general screen for new cellular TRBP interactants. Using tandem immunoaffinity purification[17] and extracts prepared from HeLa S3 cell line stably expressing a Flag-HA tagged TRBP protein (TRBP-FH), we purified TRBP and its interacting partners (Fig.1a). TRBP-associated factors were identified by mass spectrometry analysis and validated by western blot using specific antibodies (Fig.1b). As anticipated, components of miRNA machinery such as Dicer, Ago2, PACT and DDX9 were recovered in TRBP-FH immunoprecipitate, while NFkBp65, a transcription factor probed as a negative control, was not immunoprecipitated (Fig.1b). In addition to the known TRBP partners, a putative human 2'O-MTase, protein called FTSJ3 was identified. Interestingly, MAT2a, an enzyme that catalyzes the formation of the methyl donor S-adenosylmethionine (SAM), was also co-purified with TRBP/FTSJ3 complex (Fig.1b). To confirm the interaction between FTSJ3 and TRBP, reciprocal immunoprecipitation was realized in HeLa S3 cells overexpressing Flag-HA tagged FTSJ3 (Extended Data Fig.1a) and TRBP was specifically recovered in FTSJ3-FH immunoprecipitate. All these protein factors were also specifically recovered by endogenous TRBP immunoprecipitation in U937 cells infected by HIV-1 (Fig. 1c). FTSJ3 shares sequence homology with CMTR1 and CMTR2, the two human cellular 2'O-MTases involved in mRNA 2'-O-capping[18]. They all contain an FtsJ domain with a conserved catalytic KDKE motif, classical of 2'O-MTases[19]. Furthermore, its homologue in yeast, Spb1p, is responsible for 2'-O-methylation of a single internal residue, G2922, in 27S pre-rRNA[20]. FTSJ3 2'-O-methyltransferase activity was thus tested *in vitro* using capped HIV-TAR RNA as a substrate. ^{m7}G-TAR RNA was 5'-labelled and incubated for 1 hour with FTSJ3-FH immunoprecipitated proteins (IP) (Fig.1d). Nuclease P1 digestion products were analyzed on TLC chromatography plates (Fig.1e). While 5'-terminal nucleotide derived from untreated or mock IP treated TAR RNA migrates at the same level, the one derived from FTSJ3-FH treated TAR migrates faster, typical of an additional methylation. This activity is attributed to FTSJ3 since both mutant proteins, point mutated on KDKE motif or deleted of FtsJ domain show no methylation activity. FTSJ3 is also able to methylate an uncapped TAR substrate (Extended Data Fig.1b). To confirm the nature of observed methylation, FTSJ3-methylated TAR RNA was digested with tobacco acid pyrophosphatase (TAP) and released nucleotide analysed by TLC (Extended Data Fig.1c). TAP digestion of FTSJ3-FH methylated TAR, did not release any ^{m7}GMP residue, confirming that FTSJ3 induces a 2'-O-ribose methylation and not an ^{m7}G cap formation. FTSJ3 2'O-MTase activity was further

characterized by [^{3}H]CH_3 incorporation assay. Recombinant HIS-tagged FTSJ3 variants were expressed in E.coli, purified and the same amounts (Fig.1f) were incubated with in vitro transcribed, ^{m7}G-capped HIV RNA, radiolabelled [^{3}H]-SAM. Specific methyl incorporation was quantified (Fig.1g). wt-FTSJ3 induces methylation of HIV RNA, while mutant of the catalytic tetrad KDKE does not. This activity is an internal 2'-O-methylation since a synthetic 27-mer poly-rA is methylated by wt-FTSJ3, while methylation is lost when the poly-rA is already 2'-O-methylated on all 27 positions (Fig.1g). By using RNA homopolymers, we observed that FTSJ3 preferentially methylates adenosine, uridine and guanosine residues, but is not active on cytidines (Extended Data Fig.1d).

Since TRBP is a key component of miRNA pathway[21], we thus wondered if TRBP/FTSJ3 complex was also a part of the miRNA machinery. In order to better characterize these TRBP-associated complexes, glycerol gradient sedimentation of Flag-purified TRBP-FH was performed (Fig.2a). Analysis of collected fractions by western blot shows existence of 2 distinct complexes: one composed of TRBP, FTSJ3, MAT2a and DDX9 and a larger one composed of TRBP, Dicer, Ago2 and DDX9. To further characterize these species, we performed reciprocal immunoprecipitation using extracts prepared from 293T cells expressing single-tagged proteins TRBP-Flag (TRBP-F) and FTSJ3-HA (FTSJ3-H) (Fig.2b). Flag-purified TRBP-F complex was eluted using Flag peptide (Fig.3b, left panel). Eluted fraction was subjected to anti-HA immunoprecipitation to recover TRBP/FTSJ3 and their interacting partners. While TRBP co-immunoprecipitated with FTSJ3, Dicer, DDX9 and MAT2a, reciprocal immunoprecipitation of TRBP/FTSJ3 complex did not retain Dicer. Altogether, these data suggest that TRBP/FTSJ3 complex is Dicer independent. Since FTSJ3 interacts with TRBP, we verified if this complex could be recruited on HIV RNA. 293T cells were transfected with TRBP-F and FTSJ3-H and a vector expressing TAR sequence or HIV-1 molecular clone (pNL4-3). Flag and HA immunoprecipation on cell extracts led to specific recovery of TRBP and FTSJ3 proteins (Fig.2c, upper panel). Associated HIV RNAs were quantified by qRT-PCR. TRBP/FTSJ3 complex specifically retains both TAR and genomic HIV-1 RNA (Fig.2c, lower panel). To test the requirement of TRBP in FTSJ3/HIV RNA interaction, endogenous FTSJ3 was immunoprecipitated in HIV-1-infected cells where TRBP was inhibited using siRNA (Fig.2d). HIV RNA recovered in FTSJ3 immunoprecipitates was highly decreased upon TRBP knockdown. These results show that FTSJ3 interaction with HIV RNA is TRBP-dependent.

We thus evaluated the potential effect of FTSJ3 2'O-MTase activity on viral RNA and its impact on HIV expression. Since FTSJ3 is an active 2'O-MTase (Fig.1e,g), we thus searched

for potential internal 2'-O-methylated residues in HIV-1 RNA. RNA was extracted from HIV viral particles and potential 2'-O-methylated residues were assessed by RiboMethSeq analysis in two biological replicates. This high-throughput method for mapping of 2'-O-methylations in RNA is based on relative protection of neighbouring phosphodiester bond from alkaline hydrolysis[4]. Conversion of RNA fragments, obtained by random hydrolysis, to sequencing library allows precise identification of their 5'- and 3'-ends and, after mapping to the reference sequence, establishment of RNA cleavage profile using several calculation scores[4,22]. In order to rule out potential false-positive hits related to sequence- or structure-related protection against hydrolysis, we performed, in parallel, analysis of in vitro transcribed unmodified HIV-1 RNA transcripts covering the entire viral sequence (Extended Data Fig.2). Using several steps selection (see Methods) we identified 17 high-confidence 2'-O-methylated residues in HIV RNA genome (Fig.3a). The majority of internal methylation sites are A residues (15/17), highly conserved among HIV-1 major strains (Extended Data Fig.3), however no consensus sequence was found in surrounding 40 nucleotides even though distribution of sites is not random. To check if these internal methylation sites are FTSJ3-dependent, HIV viral particles were generated in 293T cells knocked out for FTSJ3 using CRISPR-Cas9 (CRISPR-Cas9-FTSJ3-HIV) (Fig.3b). Viral RNA was also purified from viruses produced in cells were FTSJ3 was knocked down using siRNA (siFTSJ3-HIV-RNA) (Extended Data Fig.5a). Comparison of scores and cleavage protection for replicates of wt-, CRISPR-Cas9-FTSJ3-, siFTSJ3-HIV RNA and unmodified transcript (Extended Data Fig.2a-q) showed that all sites present incomplete modification rate, approaching 60% of 2'-O-methylation in most cases. Several sites show highly reduced methylation rate in CRISPR-Cas9-FTSJ3-HIV RNA and, at two positions, methylation is completely absent (Fig.3c). Among those sites, we tested and validated five 2'-O-methylated residues using primer extension assay, an orthogonal validation method independent of alkaline hydrolysis. Primer extension assay at low dNTP concentration is based on the inability of AMV reverse transcriptase to process through 2'-O-methylated residue leading to a pause[22]. Primer extension was performed on mature HIV-1 RNA extracted from virions produced in 293T cells or CRISPR-Cas9-293T cells. A stop at positions 783A, 1423U, 8063A, 8403A and 8407A was specifically observed on wt-HIV-1 RNA, while a lower signal or no product was observed in HIV-1 RNA produced in FTSJ3 knocked-out cells (Fig.3d and Extended Data Fig.4).

In order to evaluate if these 2'-O-methylations could be immunomodulatory, HIV RNA extracted from viral particles produced in wt or siFTSJ3 cells (Fig.3b) were transfected into

pro-monocytic cell line U937. 16 hours later, type-1 IFN mRNAs were quantified by qRT-PCR (Fig.3e). Compared to wt-HIV RNA, HIV RNA produced in the absence of FTSJ3 induced more than 20 and 50 fold increase in IFN-α and IFN-β expression, respectively. In addition, in vitro synthesized HIV RNA methylated by recombinant FTSJ3 was transfected in U937cells and type-I IFN expression was quantified. While untreated or incubated with mutant KDKE-FTSJ3 HIV RNA transcript induced similar levels of both IFN-α and IFN-β, incubation of HIV-RNA with wt-FTSJ3 induced its methylation (Extended Data Fig.5b) and a reduced expression of type-I interferons (Fig.3f). Similarly, when a fragment of HIV RNA [8361-8461] encompassing 2 identified sites of 2'-O-methylation (8403 and 8407) was synthesized in vitro and incubated with recombinant wt-FTSJ3, it was 2'-O-methylated on A, as analyzed by digestion to 5'-mononucleotides followed by 2D TLC separation (Extended Data Fig.5c). HIV RNA fragment [8361-8461] methylated on A, induced lower expression of IFN-α and IFN-β compared to untreated or incubated with KDK-FTSJ3 mutant HIV RNA. Altogether, these data show that lower 2'-O-methylation level of HIV RNA is associated with innate immune activation.

wt-HIV and siFTSJ3-HIV viral particles were thus produced, under the same conditions, harvested in parallel, quantified and the same amounts were used to infect U937 cells for 16 hours. RNAs were purified and type-1 IFNα/β were quantified by qRT-PCR (Fig.4a). In the context of infection, siFTSJ3-HIV induced 4 to 5 fold increase in IFN-α and IFN-β expression as compared to wt-HIV. Similar results were obtained when FTSJ3/TRBP complex was inhibited by targeting TRBP in HIV producing cells (Extended Data Fig.6a). This effect is specific of FTSJ3 since viruses produced in cells knocked down for MRM2, a cellular 2'-O-MTase also called FTSJ2 involved in mitochondrial ribosomal RNA 2'-O-methylation, did not induce type-I IFN expression compared to wt-HIV (Extended Data Fig.6b). IFN induction does not result from the entry step, but from the RNA itself, since transduction of empty virus-like particles produced in siFTSJ3-293T cells did not trigger type-I IFN expression (Extended Data Fig.6c). However, infection with a virus deleted for reverse transcriptase (RT) activity produced in siFTSJ3-293T cells induced more than 2-fold increase of IFN-α and IFN-β compared to HIV produced in scramble-siRNA 293T cells (Extended data Fig.6d). Altogether these results show that unmethylated HIV RNA directly triggers IFN induction.

We thus tested if the sensing of unmethylated virus involves MDA5[1]. MDA5 or RIG-I intracellular receptors were silenced in U937 cells using specific shRNAs. Knockdown was assessed by western blot using specific antibodies (Fig.4b and extended Data Fig.7a) and further validated by control treatment either with Sendai virus, a virus shown to be detected

mainly by RIG-I, or with poly I:C, an RNA substrate sensed by both RIG-I and MDA5 (Extended Data Fig.7b). siFTSJ3-HIV and siTRBP-HIV particles were used to infect U937 cells and U937 cells silenced for MDA5 (Fig.4c). While both infections induced increased level of type-I IFN compared to wt-HIV (Fig.4a and Extended Data Fig.6a), this induction was reduced in MDA5-silenced U937 cells (Fig.4c). In contrast, RIG-I inhibition did not affect IFN-α/β induction by siFTSJ3-HIV (Extended Data Fig.7c). These results suggest that FTSJ3/TRBP complex 2'-O-methylates HIV RNA allowing its escape from MDA5 sensing.
We next assessed the immunostimulatory activity of viral particles containing low methylated HIV RNA in human primary cells isolated from healthy donors. wt- and siFTSJ3-HIV were used to infect monocyte-derived dendritic cells (MDDC) (Fig.4d-f) and monocyte-derived macrophages (MDM) (Extended Data Fig.8). Compared to wt-HIV, siFTSJ3-HIV induced strong phosphorylation of IRF-3, IRF-7 and Stat1 (Fig.4d and Extended Data Fig.5a) and induced a 2 to 6 fold increase in type-1 interferon induction in primary MDDC (Fig.4e) and MDM (Extended Data Fig.8). In a spreading infection, siFTSJ3-HIV replicated less efficiently in MDDC compared to wt-HIV (Fig.4f). Interestingly, reduced virus replication could be partially rescued in the presence of antibody targeting IFN-α/β receptor chain 2 (IFNAR2). These data show that siFTSJ3-HIV unmethylated RNA leads to innate immune sensing of the viral RNA and inhibition of HIV replication.

Altogether, our data show that TRBP recruits FTSJ3 to HIV-1 RNA and leads to its cap-adjacent and internal 2'-O-methylation at several residues. This is a new role of TRBP, independently of Dicer complex, involved in methylome of viral RNA. Recently, new techniques allowed genome-wide mapping of 2'-O-Me methylome[6], and uncovered thousand of 2'-O-methylated residues in human mRNAs. The 2'O-MTases involved and the function of these epitranscriptomic marks remain unknown. Whether TRBP-FTSJ3 complex is involved in cellular RNA modification could be of interest. This study also highlights new epitranscriptomic HIV RNA signature. Some residual methylation remains in viruses produced in FTSJ3 knockout cells suggesting the involvement of other cellular 2'O-MTases. Recently, another modification was revealed on HIV RNA, m^6A modified residues were mapped in RRE element and enhance HIV RNA export, leading to increase in HIV expression and particle release. 2'-O-methylated residues in HIV RNA, including those FTSJ3 independent, might reveal new effects or functions on viral expression and replication. We showed here that HIV-1 RNA 2'-O-methylations allow the escape from MDA5 innate immune sensing, interferon induction, and HIV expression inhibition. In addition to encoding for viral proteins that counteract restriction factors[23,24], HIV-1 hijacks cellular proteins to

modify its genome and hide from cellular host detection. This study unravelled a new way for HIV to escape innate immune system.

Methods

Plasmids

TRBP-FH, FTSJ3-FH were expressed as Flag-HA tagged proteins in the previously described MMLV-based retroviral vector pOZ[17]. FTSJ3 KDKE point mutant was generated by mutating catalytic tetrad motif $K^{31}D^{117}K^{157}$ into $A^{31}A^{117}A^{157}$ on pOZ-FTSJ3-FH using QuickChange lightning kit (Agilent technologies). FTSJ3 ΔMTase was constructed by deleting region 1-204 aa of wt FTSJ3 construct. wt FTSJ3 and FTSJ3 KDKE point mutant were cloned in SacII/NotI sites of pET47b+ (Novagen). TRBP-F was cloned in HindIII/BamHI sites of pFlag-CMV2 (Sigma). FTSJ3-H was cloned in HindIII/NotI sites of pHM6 (Roche). shMDA5 and shRIG-I were cloned in lentiviral pLKO.1 vector.

Identification TRBP associated factors

TRBP associated complex was purified from HeLa S3 cells stably expressing double tagged Flag-HA TRBP human protein (TRBP-FH) by two-step affinity chromatography as previously described[17]. Briefly, cell extracts from $2x10^9$ HeLa S3 cells (mock) or HeLa S3-TRBP-FH cells were subjected to a first immunoprecipitation using anti-Flag agarose beads. Elution was performed under native conditions by competition with a Flag peptide. Eluted proteins were submitted to a second immunoprecipitation using anti-HA agarose beads. HA peptide eluted proteins were analyzed on a 4-12 % SDS page gel followed by silver or colloidal blue staining and subsequently analyzed by tandem mass spectrometry at the Taplin Biological Mass Spectrometry facility (Harvard Medical School, Boston, MA). Immunoprecipitation of endogenous TRBP and FTSJ3 were performed using anti-TRBP (Proteintech, 15753-1-AP); anti FTSJ3 (Bethyl, A304-199A) or a purified rabbit IgG antibody as control (Bethyl, P120-201). Western blots were revealed using specific antibodies recognizing TRBP (Proteintech, 15753-1-AP or ThermoFisher Scientific, LFMA0209); FTSJ3 (Abgent, WA-AP12057 or Bethyl, A304-199A); HA (Roche, 11867423001); Flag (Sigma; F1804); MAT2A (Novus, NB110-94158); Dicer (Bethyl, A301-936); Ago2 (abcam, ab32381); PACT (Bethyl, A302-017); DDX9 (Bethyl A300-854); NFκB p65 (Merck, 06-418); HIV-1 p24 (AIDS reagent program, 4250), phospho-IRF3 (abcam, ab76493); phospho-

IRF7 (cell signaling, 12390); phospho-Stat1(cell signaling, 9167); ERK1/2 (cell signaling, 4695). Western blots following endogenous immunoprecipations were revealed using EasyBlot Kit (GeneTex).

Recombinant protein purification

pET47b-wt FTSJ3 and pET47b-FTSJ3 KDKE constructs were transformed in Rosetta-gami2(DE3)pLysS (Novagen). HIS-tagged proteins were purified as previously described[25]. Additional washing steps of Ni-NTA beads were added using successively 1 M NaCl, 0.5 M, 0.25 M and 0.125 M NaCl in PBS before elution to eliminate bacterial RNA that could be retained and interfere with the activity assay. Purified proteins were further dialyzed against storage buffer (20 mM Tris-HCl, pH 8, 150 mM NaCl, 1 mM DTT and 50% glycerol) analyzed and on-gel quantified by Coomassie blue and western blot then aliquoted and stored at -80°C.

***In vitro* RNA 2'-O-methylation assays**

TAR RNA was transcribed *in vitro* and radiolabelled with $^{\alpha 32}$P-GTP using ScriptCap capping system following manufacturer's instructions (Epicentre). TAR was also ^{m7}G-capped, by adding S-adenosyl methionine in the reaction (^{m7}G-TAR). Uncapped and capped TAR RNAs were used as substrates. HeLa S3, S3-FTSJ3-FH, S3-FTSJ3-KDKE-FH or S3-FTSJ3ΔMTase-FH cell extracts (from 10^7 cells) were subjected to Flag/HA immunoprecipitations. HA immunoprecipitates were resuspended in 100 µl volume and tested for their 2'-O-methyltransferase activity as previously described[26]. Briefly, methylation assay was performed on 0.5 µg of TAR RNA, with 10 µl of immunoprecipitated proteins and resuspended in assay buffer (50 mM Tris-HCl pH7.9, 2 mM DTT, 50 µM SAM and RNase inhibitor) for 1 hour at 30°C. RNAs were purified by phenol/chloroform, immunoprecipitated and split in two equal parts. One part was resuspended in 50 mM NaOAc and digested with Nuclease P1 (USBiological) for 3 hours. The other part was treated with Tobacco acid pyrophosphatase (Epicentre) for 1 hour at 37°C. Digested products were spotted on TLC plates (PEI-cellulose) and developed with 0.3 M or 0.45 M ammonium sulfate buffer respectively. Labelled cap structures were visualized by autoradiography.

FTSJ3 methyltransferase activity was further analyzed by [^{3}H]CH_3 incorporation assay as described previously[12]. Briefly, 3 µM of purified wt $_{HIS}$FTSJ3 or mutant-KDK- $_{HIS}$FTSJ3 were incubated with 6.6 µM of purified synthetic RNAs (A_{27}, $(Am)_{27}$, U_{27}, G_{27}, C_{27}, (biomers)) or 0.33 µM of purified in vitro transcribed HIV RNA and 0.4 µM of [^{3}H]-SAM (Perkin Elmer)

in MTase buffer (50 mM Tris-HCl pH 8, 3.3 mM DTT). Reactions were incubated for 5h at 30°C and stopped by a 20-fold dilution in cold water. Samples were transferred to DEAE filtermats using a Filtermat Harvester (Packard Instruments). DEAE filters were washed twice with 10 mM ammonium formate pH 8, twice with water and once with 96% ethanol. They were then soaked with liquid scintillation fluid (Perkin Elmer), and the [^{3}H]CH_3 transfer to the RNA substrates was measured (cpm) by using a Wallac MicroBeta TriLux Liquid Scintillation Counter13 (Perkin Elmer).

In vitro RNA methylation assay was performed as described in Grosjean et al., 2007. Digested 5'-monophosphate nucleotides were loaded on cellulose TLC plates (Merck, 105716) and 2D migration was done in N1/N2 or N1/R2 solvents as described in Grosjean et al., 2007.

Cells

HEK-293T and HeLa S3 cells were grown in Dulbecco modified Eagle medium (DMEM), U937 cells in RPMI medium at 37°C in 5% CO_2. Medium was supplemented with heat-inactivated fetal calf serum (FCS) and antibiotics. 293T cells knocked-out for FTSJ3 were generated by deleting FTSJ3 genomic region 2544-4923 (ENSG00000108592) using CRISPR Cas9 technology as previously described[27]. Briefly, gRNA-1 (GGCTAAGACCGTTACTGAAT) was cloned in pLentiCRISPRv2GFP and gRNA-2 (CAAGACGGCTCGGATGCCGG) in pLentiCRISPRv2. Pseudotyped viruses were produced and transduced into 293T cells. 48 hours post-transduction, puromycin was added, and 72 hours later GFP-positive cells were sorted and plated at limited dilution. Grown clones were screened using PCR primers within FTSJ3 MTase domain to assess complete deletion and by western blot using two different antibodies recognizing FTSJ3. Human primary monocyte-derived dendritic cells (MDDC) and primary monocyte-derived macrophages (MDM) were prepared from buffy coats from healthy donors obtain from "Etablissement Français du Sang" (EFS) as previously described[28]. Briefly, monocytes were purified from total peripheral blood mononuclear cells after Ficoll density centrifugation using CD14 selection magnetic beads (Miltenyi Biotec). Monocytes were resuspended in RPMI medium complemented with 5% human serum and differentiated into MDM using 50 ng/ml GMCSF for 5 days or into MDDC using 50 ng/ml of GM-CSF and 10 ng/ml of IL-4 for 6 days. Recombinant human granulocyte-macrophage colony-stimulating factor (GM-CSF) and recombinant human

interleukin-4 (IL-4) were purchased from Immunotools. Derived cells were checked by FACS analysis.

Viral productions

HEK-293T cells were transfected using Interferin with siRNA targeting FTSJ3 (siFTSJ3 GCCAACCUGUGGUUCUCAA); or TRBP (siTRBP GCCUGAUGAUGACCACUUC); MRM2 (siMRM2 GCUGGUGUGUGUUUCCUUU) or non-targeting sequence (siScramble GCGCGCUUUGUAGGAUUCG) following manufacturer's instructions (Polyplus). 16 hours later, cells were transfected with a second round of siRNA. 24 hours later, cells were then transfected with 10 µg of HIV molecular clone pNL4-3 or HIV molecular clone using standard phosphate calcium transfection protocol. The CCR5-tropic wild-type NL4-3, Ba-L env, called HIV-BaL, and mutant RT-HIV-BaL(D185E RT) were kindly provided by Greg Towers[29]. Medium was replaced 16 hours post-transfection. 36 hours post transfection, supernatants were harvested, filtered using 0.45 µm filters and ultracentrifuged through a 20% sucrose cushion. Virion productions were quantified by RT activity and p24 ELISA (Helvetica Health Care). Ratio of encapsidated viral RNA genome versus Gag capsid was quantified to assess virion quality production in mock and siRNA-treated 293T cells. Protein expression knock-down was assessed by western blot using specific antibodies before molecular clone transfection and after harvesting virions in producer cells. When indicated virus was VSV-G pseudotyped using additional 1µg pMD2G plasmid. Virus-like particles were produced as previously described[28]. Sendai virus was purchased from ATCC.

In vitro HIV-1 RNA transcripts

pNL4-3 HIV sequences (GenBank accession AF324493) were cloned as 2 overlapping fragments (455-5120; 3895-9625) in pSC-B-T7 vector (Agilent) and as 8 overlapping fragments (455-1350; 1300-2840; 2790-3945; 3895-5120; 5050-6330; 6280-7250; 7180-8275; 8207-9625) in pGEM T7 vector (Promega). 500 ng of each linearized vector was used as a template for in vitro transcription using T7 AmpliScribe flash kit (Epicentre). HIV DNA fragment [8816-8915] was synthesized with a T7 promoter sequence upstream and used as a template to synthesize HIV RNA [8362-8461]. RNA was treated with DNase I, purified with phenol/chloroform and precipitated. Purified RNA were quantified using Nanodrop and visualized on agarose gel. When indicated, in vitro synthesized RNA was ^{m7}G-capped using Epicentre kit.

RiboMethSeq library construction

Full length HIV-1 genomic RNA was purified from HIV virions (pNL4-3) produced in wt, CRISPR-Cas9-FTSJ3 or FTSJ3 siRNA-treated cells as previously described[30]. Briefly, concentrated virions were treated with 1 mg/ml subtilisin (Sigma) and purified by centrifugation on a 20% sucrose cushion. Viral particle RNA was purified using Trizol LS (ThermoFisher Scientific) and ethanol precipitated. Full length HIV genome was further purified by size selection using E.gel size select (ThermoFisher Scientific). Purified RNA was quantified by fluorometry using Qubit. 10 ng of viral RNA extracted from viral particles or a mix in equal amounts of *in vitro* transcribed RNA were submitted to alkaline treatment and converted to library using NEBNext Small RNA library kit as previously described[4]. Library were multiplexed and subjected to high-throughput sequencing using Illumina HiSeq 1000 in a single read SR50 mode.

RiboMethSeq bioinformatic analysis

Analysis of 2'-O-methylations present in HIV-1 RNA was performed using previously published RiboMethSeq protocol[4]. 9 samples were analyzed in parallel: 2 mixes of unmodified in vitro HIV-1 RNA transcripts, 2 biological replicate samples of wt-HIV-1 RNA extracted from virions; 2 samples of RNA isolated from HIV-1 virions produced in cells treated with siRNAs targeting FTSJ3 and 3 samples of RNA isolated from HIV-1 virions produced in cells knocked out for FTSJ3 using CRISPR-Cas9. The systematic use of biological replicates allowed to estimate the variability of primary data. First of all, the alkaline cleavage profile for each sample was calculated by alignment of trimmed short HIV-1 RNA reads to the reference sequence (pNL4-3, AF324493) and counting of their 5'- and 3'-extremities. From the cleavage profile we calculated previously described RiboMethSeq scores (ScoreMean, Score A, Score B and Score C). Using this approach, we tentatively identified over 200 locations in HIV-1 RNA which showed affected cleavage profile and an important decrease of RNA protection at certain positions. Since RNA protection from cleavage can result either from the presence of 2'-O-methylated nucleotides or from structural and/or sequence context effects, we compared cleavage profile of unmodified in vitro HIV-1 transcripts and wt-HIV-1 RNA extracted from virions. The overall cleavage profile obtained for in vitro transcripts was remarkably similar to wt-HIV-1 RNA, indicating that under fragmentation conditions used in the experiment (96°C), only a few elements of residual RNA structure may influence observed cleavage profile. Median absolute difference for ScoreMean is only 0.054, while the average difference for Score C is 0.081 for all tested HIV-1 positions,

showing a low bias in fragmentation. Comparison of scores values between HIV-1 RNA samples and in vitro transcripts allowed to remove potential false positive hits already present in unmodified RNA. Out of 221 positions showing important cleavage protection (combination of ScoreMean>0.9, Score A>0.5, Score B>5, Score C>0.75), 174 are present already in unmodified RNA, indicating that false-positive rate resulting from structure or sequence effects for average RNA is close to 1.9%. Similar false-positive rates were also observed for unmodified in vitro transcripts of yeast and human rRNAs[4]. The remaining 47 sites were further analyzed by close inspection of local cleavage profile around the protected site. This analysis allowed retaining 16 positions showing difference of cleavage at a single position, and not a global profile change. Since the highest values of protection scores observed in wt-HIV-1 RNA mostly correspond to false-positive hits, we investigated other positions showing moderate protection (ScoreMean> 0.4/low Score A/Score B>1/Score C>0.5) but with a clear decrease of Score C between wt-HIV-1 RNA and in vitro transcripts. Over 80 positions fulfilling these criteria were found, we retained only 21 showing consistent decrease of Score C >0.4 between two biological replicates and with wt-HIV-1 Score C>0.5. For these sites, a closer visual inspection was performed as described previously[4] : sites showing a global change in cleavage profile or a high protection in in vitro transcript and low in wt-HIV-1 RNA (only 7 sites) were eliminated. The majority of sites show an important global decrease of protection in in vitro transcript compared to naturally matured HIV-1 RNA. This filtering allowed the selection of only 17 sites in HIV-1 RNA satisfying these strict selection criteria (Fig.3). The great majority of these sites are A residues (with 2 Um exceptions) and most of them also show a FTSJ3 dependence, since their protection strongly decreases in HIV-1 RNA produced in cells knocked out for FTSJ3.

Primer extension assay

RT primers (for 783: cccccactgtgtttagcatggtat; for 1423: tgccacaattgaaacacttaacagtc; for 8063 : gtcccagaagttccacaatcct and for 8403/8407: gctacttgtgattgctccatgt) were radiolabeled with γ^{32}P-ATP using T4 polynucleotide kinase and used to check 2'O-Me status of the corresponding residues on HIV genome. 250 ng of RNA was hybridized with ^{32}P radiolabeled RT primer (10^5 cpm) in 1X RT buffer (MP Biomedicals) in a total volume of 2.5 µl. The mix was incubated for 40 seconds at 96°C, chilled on ice, incubated for 10 minutes at 65°C, then chilled for 1 minute on ice. dNTP were added at a concentration of 1 mM (high) or 0.004 mM (low) and RT was initiated by 0.5 unit of AMV RT (MP Biomedicals) in a final volume of 5 µl. Sequencing reaction was run in parallel using wt-HIV RNA as a template in the same

conditions, dNTP mix was replaced by 0.04 mM dNTP complemented with each of the four ddNTP (0.05 mM). RT reactions were conducted at 42°C for one hour and terminated by adding 4 µl of stop solution (95 % formamide, 20 mM EDTA, 0.05% bromophenol blue, 0.05% xylene cyanol). RT products were denatured at 96°C for 2 minutes and loaded on a 7% TBE-acrylamide-urea sequencing gel. Gel was dried one hour at 80°C, exposed overnight on a PhosphorImager plate and scanned using Amersham Typhoon imager (GE Healthcare).

RNA immunoprecipitation

Cells were harvested 16 hours after pTAR or pNL4-3 transfection, lysed for 15 min in RIP buffer (20 mM Hepes-KOH, pH 7.5, 150 mM NaCl, 2.5 mM $MgCl_2$, 250 mM Sucrose, 0.05% (v/v) NP40, 0.5% (v/v) Triton X-100) containing RNasin (Promega) and 1 mM DTT, and centrifuged to pellet debris. Supernatants were incubated 4 hours with anti-Flag agarose beads at 4°C. After 5 washes, immunoprecipitated material was eluted using 200 ng/ml of Flag peptide. Eluates were subjected to a second immunoprecipitation using anti-HA agarose beads for 1 hour. Flow through were recovered and analyzed at the protein and RNA level. Immunoprecipitates were washed 5 times with RIP buffer, 1/10 was used for western blot analysis while 9/10 were used for RNA purification. Nucleic acids were extracted with phenol/chloroform/isoamyl alcohol, precipitated, ethanol-washed and resuspended in RNAse-free water. Total RNA was DNase I treated. After heat inactivation, RNA was reverse-transcribed using SuperScript kit (Thermo Fisher Scientific). RT products were PCR-amplified on LightCycler 480 (Roche) successively using specific primers: TAR forw GGGTCTCTCTGGTTAGA; TAR rev GGGTTCCCTAGTTAGCC, HIV forw GACGCTCTCGCACCCATCTC; HIV rev CTGAAGCGCGCACGGCAA known to amplify unspliced full length HIV RNA genome [31]. RNAs were also purified in the input extracts and submitted to qRT-PCR. As a control, actin and GAPDH were also quantified in both input and immunoprecipitated material. Both are not enriched in specific immunoprecipitated TRBP/FTSJ3 complex.

RNA transfections

Viral particle RNA was purified using Trizol LS (Thermo Fisher Scientific) and ethanol precipitated. Purified viral RNA or in vitro synthesized RNA were transfected using TransIT mRNA transfection kit (Mirus Bio) according to manufacturer's instructions. 1 µg of purified viral RNA was transfected into $5x10^5$ U937 cells.

Infections

U937 cells infection was performed by adding equivalent amounts of p24 of HIV virus produced in wt or siRNA treated 293T cells. For spreading infection, MDDC were preincubated with virus-like particles expressing Vpx (VLP-Vpx) 2 hours before infection as previously described[28]. For interferon neutralizing experiments, MDDC were incubated with 1µg/ml of anti-human IFN-α/β receptor (PBL, 21385) or control IgG2A antibody (R&D system, MAB003) two hours before infection as previously described[29].

Type-I interferons quantification

RNA were purified 16 hours post-transfection or post-infection using Trizol reagent and reverse-transcribed using SuperScript (ThermoFisher Scientific). RT products were PCR-amplified LightCycler 480 (Roche) successively using specific primers: IFN-α (IFN-α forw: GCTTTACTGATGGTCCTGGTGGTG, IFN-α rev: GAGATTCTGCTCATTTGTGCCAG); IFN-β (IFN-β forw: GAATGGGAGGCTTGAATACTGCCT, IFN-β rev: TAGCAAAGATGTTCTGGAGCATCTC); and actin (actin forw: AACCCAGCCACACCACAAAG actin rev: CACTGACTTGAGACCAGTTGAATAAAA); GAPDH (GAPDH forw: CTGGCGTCTTCACCACCATGG; GAPDH rev: CATCACGCCACAGTTTCCCGG).

References

1 Zust, R. *et al.* Ribose 2'-O-methylation provides a molecular signature for the distinction of self and non-self mRNA dependent on the RNA sensor Mda5. *Nature immunology* **12**, 137-143, doi:10.1038/ni.1979 (2011).

2 Daffis, S. *et al.* 2'-O methylation of the viral mRNA cap evades host restriction by IFIT family members. *Nature* **468**, 452-456, doi:10.1038/nature09489 (2010).

3 David, R. Immune evasion: Gm18, a bacterial 'invisibility cloak'. *Nature reviews. Microbiology* **10**, 238-239, doi:10.1038/nrmicro2767 (2012).

4 Marchand, V., Blanloeil-Oillo, F., Helm, M. & Motorin, Y. Illumina-based RiboMethSeq approach for mapping of 2'-O-Me residues in RNA. *Nucleic acids research* **44**, e135, doi:10.1093/nar/gkw547 (2016).

5 Motorin, Y. & Helm, M. RNA nucleotide methylation. *Wiley Interdiscip Rev RNA* **2**, 611-631, doi:10.1002/wrna.79 (2011).

6 Dai, Q. *et al.* Nm-seq maps 2'-O-methylation sites in human mRNA with base precision. *Nat Methods*, doi:10.1038/nmeth.4294 (2017).

7 Shuman, S. What messenger RNA capping tells us about eukaryotic evolution. *Nature reviews. Molecular cell biology* **3**, 619-625, doi:10.1038/nrm880 (2002).

8 Schoggins, J. W. *et al.* A diverse range of gene products are effectors of the type I interferon antiviral response. *Nature* **472**, 481-485, doi:10.1038/nature09907 (2011).

9 Schuberth-Wagner, C. *et al.* A Conserved Histidine in the RNA Sensor RIG-I Controls Immune Tolerance to N1-2'O-Methylated Self RNA. *Immunity* **43**, 41-51, doi:10.1016/j.immuni.2015.06.015 (2015).
10 Decroly, E., Ferron, F., Lescar, J. & Canard, B. Conventional and unconventional mechanisms for capping viral mRNA. *Nature reviews. Microbiology* **10**, 51-65, doi:10.1038/nrmicro2675 (2012).
11 Dong, H. *et al.* 2'-O methylation of internal adenosine by flavivirus NS5 methyltransferase. *PLoS pathogens* **8**, e1002642, doi:10.1371/journal.ppat.1002642 (2012).
12 Martin, B. *et al. Nucleic Acids Res* **150** (2018).
13 Gehrig, S. *et al.* Identification of modifications in microbial, native tRNA that suppress immunostimulatory activity. *The Journal of experimental medicine* **209**, 225-233, doi:10.1084/jem.20111044 (2012).
14 Jockel, S. *et al.* The 2'-O-methylation status of a single guanosine controls transfer RNA-mediated Toll-like receptor 7 activation or inhibition. *The Journal of experimental medicine* **209**, 235-241, doi:10.1084/jem.20111075 (2012).
15 Gatignol, A., Buckler-White, A., Berkhout, B. & Jeang, K. T. Characterization of a human TAR RNA-binding protein that activates the HIV-1 LTR. *Science* **251**, 1597-1600 (1991).
16 Benkirane, M. *et al.* Oncogenic potential of TAR RNA binding protein TRBP and its regulatory interaction with RNA-dependent protein kinase PKR. *The EMBO journal* **16**, 611-624, doi:10.1093/emboj/16.3.611 (1997).
17 Nakatani, Y. & Ogryzko, V. Immunoaffinity purification of mammalian protein complexes. *Methods in enzymology* **370**, 430-444, doi:10.1016/S0076-6879(03)70037-8 (2003).
18 Werner, M. *et al.* 2'-O-ribose methylation of cap2 in human: function and evolution in a horizontally mobile family. *Nucleic acids research* **39**, 4756-4768, doi:10.1093/nar/gkr038 (2011).
19 Hodel, A. E., Gershon, P. D., Shi, X. & Quiocho, F. A. The 1.85 A structure of vaccinia protein VP39: a bifunctional enzyme that participates in the modification of both mRNA ends. *Cell* **85**, 247-256 (1996).
20 Lapeyre, B. & Purushothaman, S. K. Spb1p-directed formation of Gm2922 in the ribosome catalytic center occurs at a late processing stage. *Mol Cell* **16**, 663-669, doi:10.1016/j.molcel.2004.10.022 (2004).
21 Chendrimada, T. P. *et al.* TRBP recruits the Dicer complex to Ago2 for microRNA processing and gene silencing. *Nature* **436**, 740-744, doi:10.1038/nature03868 (2005).
22 Helm, M. & Motorin, Y. Detecting RNA modifications in the epitranscriptome: predict and validate. *Nature reviews. Genetics* **18**, 275-291, doi:10.1038/nrg.2016.169 (2017).
23 Blanco-Melo, D., Venkatesh, S. & Bieniasz, P. D. Intrinsic cellular defenses against human immunodeficiency viruses. *Immunity* **37**, 399-411, doi:10.1016/j.immuni.2012.08.013 (2012).
24 Laguette, N. & Benkirane, M. How SAMHD1 changes our view of viral restriction. *Trends in immunology* **33**, 26-33, doi:10.1016/j.it.2011.11.002 (2012).
25 Bennasser, Y. *et al.* Competition for XPO5 binding between Dicer mRNA, pre-miRNA and viral RNA regulates human Dicer levels. *Nat Struct Mol Biol* **18**, 323-327, doi:10.1038/nsmb.1987 (2011).
26 Belanger, F., Stepinski, J., Darzynkiewicz, E. & Pelletier, J. Characterization of hMTr1, a human Cap1 2'-O-ribose methyltransferase. *The Journal of biological chemistry* **285**, 33037-33044, doi:10.1074/jbc.M110.155283 (2010).

27 Bauer, D. E., Canver, M. C. & Orkin, S. H. Generation of genomic deletions in mammalian cell lines via CRISPR/Cas9. *J Vis Exp*, e52118, doi:10.3791/52118 (2015).
28 Laguette, N. *et al.* SAMHD1 is the dendritic- and myeloid-cell-specific HIV-1 restriction factor counteracted by Vpx. *Nature* **474**, 654-657, doi:10.1038/nature10117 (2011).
29 Rasaiyaah, J. *et al.* HIV-1 evades innate immune recognition through specific cofactor recruitment. *Nature* **503**, 402-405, doi:10.1038/nature12769 (2013).
30 Watts, J. M. *et al.* Architecture and secondary structure of an entire HIV-1 RNA genome. *Nature* **460**, 711-716, doi:10.1038/nature08237 (2009).
31 Brussel, A. & Sonigo, P. Evidence for gene expression by unintegrated human immunodeficiency virus type 1 DNA species. *J Virol* **78**, 11263-11271, doi:10.1128/JVI.78.20.11263-11271.2004 (2004).

Figures legends

Figure 1: FTSJ3 2'-O-methyltransferase interacts with TRBP. a, TRBP-FH was immunoprecipitated from HeLa S3 (mock) or HeLa S3-TRBP-FH cell extracts using tandem immunoaffinity purification. Eluted proteins were analyzed on SDS-PAGE gel and silver stained. Major interactants were identified by mass spectrometry and further confirmed by western blot using specific antibodies in **b**. **c**, U937 cells were infected with HIV-1 and subjected to endogenous immunoprecipitation using anti-TRBP antibodies or an IgG irrelevant antibody used as control. Whole cell extracts and immuno-precipitated complexes were analysed by WB using the indicated antibodies. **d**,**e**, FTSJ3 methylation activity was assessed in vitro using ^{m7}G-TAR RNA as a substrate. Radiolabeled ^{32}P-^{m7}G-TAR was incubated for 1 hour at 30°C with equal amounts of Flag/HA immunoprecipitated FSTJ3-FH, KDKE point mutant FSTJ3-FH, ΔMTase-FSTJ3-FH or mock IP blotted in **d**, RNA were then treated with nuclease P1 for 3 hours, and released caps were analyzed by TLC chromatography in 0.3 M ammonium sulfate buffer. Plate was dried and exposed by autoradiography. **f, g**, Purified recombinant $_{HIS}$FTSJ3 wt or catalytic mutant KDKE blotted in **f** were incubated with in vitro transcribed and ^{m7}G-capped HIV-1 RNA in presence of radiolabeled [^{3}H]-SAM. MTase activity was determined by filter binding assay. wt-$_{HIS}$FTSJ3 internal MTase activity was further assessed on synthetic 27 nucleotide-long polyA RNAs (A27) or with all residues 2'O-methylated RNA ($(Am)_{27}$). The background obtained in the absence of exogenous RNA was subtracted. *n*=3, results shown as the mean ± s.d

Figure 2: FTSJ3/TRBP complex is recruited to HIV-1 viral RNA through TRBP and is different from TRBP/Dicer complex. a, Flag-purified TRBP-FH-associated complexes were separated by centrifugation through a 15%–35% glycerol gradient and analyzed by western blot using specific antibodies. **b**, 293T cells cotransfected with two vectors expressing TRBP-F and FTSJ3-H were submitted to Flag/HA immunoprecipitation. Eluted TRBP-F (left panel) and TRBP/FTSJ3-H (right panel) associated factors were analyzed by western blot. **c**, TRBP-F and FTSJ3-H were cotransfected with a TAR-expressing vector (left panels) or pNL4-3 HIV-1 molecular clone (right panels). Following Flag/HA immunoprecipitations, HA eluted proteins were analyzed by western blot, while associated RNA were analyzed by qRT-PCR using specific primers. **d**, 293T cells were transfected with scramble (-) or siTRBP, infected with VSV-G-pseudotyped HIV-1 and whole cell extracts were subjected to endogenous TRBP immunoprecipitation. Whole cell extracts and immune-precipitated complexes were analyzed by western blot (left panels) and associated HIV-1 RNA genome was quantified by specific qRT-PCR.

Figure 3: HIV RNA isolated from viral particles is internally 2'-O-methylated by FTSJ3. a, Viral RNA was purified from viral particles and submitted to RiboMethSeq analysis. 17 high-confidence 2'-O-methylated sites were mapped on HIV-1 pNL4-3 RNA (see Extended Data Fig.2). **b,** HIV viruses were produced in 293T cells knocked-out for FTSJ3 using CRISPR-Cas9 technology (CRISPR-Cas9-FTSJ3). **c**, Normalized methylation levels (ScoreC normalized to in vitro HIV-1 transcript) of detected 2'-O-methylated sites in wt-HIV-1 RNA and in CRISPR-Cas9-FTSJ3-HIV-1 RNA extracted from viral particles. n=2 for wt-HIV-1 RNA and n=3 for CRISPR-Cas9-FTSJ3-HIV-1 RNA, individual data points are shown **d**, Primer extension assay realized on same amounts of HIV RNA isolated from viral particles produced in wt or CRISPR-Cas9-FTSJ3 cells using high and low concentrations of dNTP (see Extended Data Fig.4). Validated 2'-O-methylated positions are marked by an arrow. **e**, RNA purified from wt- and siFTSJ3-HIV viral particles were transfected in U937 cells. 16 hours later, IFN-α and IFN-β expression were quantified by qRT-PCR. $n \geq 3$, results shown as the mean ± s.d. ****$p \leq 0.0001$ by two-tailed Student's t-test. **f**, In vitro synthesized HIV-1 RNA, or HIV-1 RNA fragment [8362-8461] were methylated in vitro with wt or mutant-KDKE FTSJ3 and transfected in U937 cells. 24 hours later, IFN-α and IFN-β expression were quantified by qRT-PCR. $n \geq 3$, results shown as the mean ± s.d. ***$p \leq 0.001$, **$p \leq 0.01$, *$p \leq 0.05$ by two-tailed Student's t-test.

Figure 4: HIV viral particles produced in FTSJ3 knock-down cells induce type-I interferons expression that inhibits HIV-1 expression. a, U937 cells were infected with the same amounts of wt-HIV and siFTSJ3-HIV viruses. 16 hours later, IFN-α and IFN-β expression was quantified by qRT-PCR **b**, Inhibition of MDA5 using shRNA in U937 assessed by western blot. **c**, Type-I interferons expression in U937 or U937-shMDA5 cells infected by siFTSJ3-HIV or siTRBP-HIV viral particles. IFN-α and IFN-β were quantified by qRT-PCR 16 h.p.i. **d**, MDDC were infected with wt- or siFTSJ3 HIV-BaL, 4 h.p.i cell extracts were analyzed by western blots using indicated antibodies. **e**, 16 h.p.i., IFN-α and IFN-β were quantified using qRT-PCR. $n \geq 3$, results shown as the mean ± s.d. ****$p \leq 0.0001$; **$p \leq 0.005$ by two-tailed Student's *t*-test **f**, Kinetic of infection of MDDC with siFTSJ3 or wt-HIV-BaL in the absence or presence of IFNAR2 or a control antibody. Cells were pretreated with Vlp-Vpx to allow viral replication. n=3, results shown as the mean ± s.d.

Extended Data Figure 1: FTSJ3 is a human 2'-O-methyltransferase.

a, Reciprocal immunoprecipitation was performed on HeLa S3 cells expressing Flag/HA double tagged FTSJ3 protein (FTSJ3-FH). Eluates were analyzed using anti-HA and anti-TRBP antibodies. **b**, FTSJ3 methylation activity was assessed in vitro using TAR RNA as a substrate. Radiolabeled ^{32}P-TAR was incubated for 1 hour at 30°C with equal amounts of Flag/HA immunoprecipitated FSTJ3-FH or mock IP blotted in Fig 1d. RNA were then treated with nuclease P1 for 3 hours, and released caps were analyzed by TLC chromatography migration using 0.3 M ammonium sulfate buffer. Plate was dried and exposed by autoradiography. **c**, Products from in vitro mock and FTSJ3-FH TAR methylation were digested with tobacco acid pyrophosphatase (TAP). As a control, ^{32}P-^{m7}G-TAR was also digested with TAP, to release ^{m7}GMP residue. Products are analyzed on TLC plate developed with 0.45M ammonium sulfate buffer. **d**, Purified recombinant FTSJ3 was incubated without exogenous RNA (-) or with homopolymeric synthetic 27-mer RNAs A27, U27, G27 and C27 and associated MTase activity was determined by filter binding assay. The background obtained in absence of exogenous RNA was subtracted. $n = 3$, results shown as the mean ± s.d. **p ≤ 0.005 by two-tailed Student's *t*-test.

Extended data Figure 2: RiboMethSeq analysis of 2'-O-methylated sites detected in HIV RNA isolated from viral particles:

a-q, For each of the seventeen 2'-O-methylated sites, RiboMethSeq data are presented from top to bottom: *Top panel*: Superposed relative local cleavage profiles for four conditions

(transcript, wt-HIV-1 RNA, siFTSJ3-HIV-1 RNA and CRISPR-Cas9-FTSJ3-HIV-1 RNA). *Middle panel*: Relative local cleavage profile for in vitro T7 transcript of HIV-1 RNA, for wt-HIV-1 RNA, siFTSJ3-HIV-1 RNA and CRISPR-Cas9-FTSJ3-HIV-1 RNA extracted from virions. Individual points for biological replicates are shown, position numbers are indicated on the bottom. *Lower panel*: Variations and absolute values of RiboMethSeq scores (ScoreC, ScoreMean, Score A and Score B) for methylated position. ScoreC, ScoreMean and Score A generally vary from 0 to 1 (negative values are possible), while Score B may be > 1 for highly methylated positions in RNA. In RiboMethSeq the protection caused by 2'-O-methylation appears at the 3'-neighboring position in RNA. For simplicity, -1 shift was applied to numbering here, thus increased protection signal falls exactly to 2'-O-methylated nucleotide. Individual points for biological replicates are shown; n=2 or n=3

Extended Data Figure 3: Conservation frequency of the seventeen identified 2'-O-methylated residues among major HIV-1 subtypes and circulating recombinant forms. The 17 sites of 2'O-methylation identified on HIV-1 molecular clone, pNL4-3, were aligned to up to 2436 sequences of major HIV-1 subtypes and circulating recombinant forms sequences available on Los Alamos HIV database (http://www.hiv.lanl.gov/). The number of sequences analyzed for each position and the conservation frequency are presented in the table.

Extended Data Figure 4: Validation of 783A, 1423U, 8063A, 8403A and 8407A 2'-O-methylations using primer extension assay. HIV-1 RNA isolated from viral particles produced in mock cells (wt) or cells knocked-out for FTSJ3 using CRISPR-Cas9 (CRISPR-Cas9-FTSJ3) were subjected to primer extension assay using specific radiolabeled primers. Extension assay was realized in high (1,3) and low concentrations (2,4) of dNTP as indicated. Sequencing experiment was run side by side using wt-HIV RNA as a template (4-8). Primer extension products were analyzed on acrylamide-urea sequencing gel and visualized by autoradiography. 2'O-methylated position and stop is indicated by an arrow.

Extended Data Figure 5: Characterization of HIV-1 RNA transfected in U937 cells.
a, HIV viruses were produced in 293T cells transfected with FTSJ3 siRNAor a control non-specific siRNA (scramble). FTSJ3 inhibition was assessed by western blot. **b**, Purified recombinant $_{HIS}$FTSJ3 wt or catalytic mutant KDKE was incubated with in vitro transcribed HIV-1 RNA in presence of radiolabeled [^{3}H]-SAM and MTase activity was determined by

filter binding assay (FBA). **c**, Purified recombinant wt-FTSJ3 was incubated without exogenous RNA or with the [8362-8461] HIV RNA fragment and MTase activity was determined by FBA (left panel) or 2D TLC separation (right panel). FBA results were normalized by subtracting the background obtained in absence of exogenous RNA. 2D TLC separation of 5'-[^{32}P]-NMPs resulted from nuclease P1 hydrolysis of HIV RNA transcript [8362-8461] radiolabeled with [α-^{32}P]ATP and incubated with wt-FTSJ3 or mutant KDKE-FTSJ3 recombinant proteins. Migration was performed in N1/N2 or N1/R2 combination of solvents as described in Methods section. Positions of unmodified AMP (pA), 2'-O-methyl AMP (pAm) and inorganic phosphate (Pi) are indicated.

Extended Data Figure 6 : HIV viral particles produced in TRBP knock-down cells induce type-I interferons expression while viruses produced in siMRM2 knocked-down, and siFTSJ3-emply virus-like particles do not.

a, 293T cells were transfected with siRNA targeting TRBP (siTRBP) (in **a**), FTSJ3 (siFTSJ3) or MRM2 (siMRM2) (in **b**) or a control non-specific siRNA (scramble). 16 hours post-transfection, cells were further transfected with pNL4-3 HIV molecular clone. Viruses were harvested 48 hours later and quantified for RT, p24 and packaged viral RNA. Protein inhibition was assessed by western blot (upper panels) U937 cells were infected with same amounts of viruses produced in cells treated with scramble siRNA (wt-HIV) or siTRBP, siFTSJ3, siMRM2 as indicated. 16 hours later, IFN-α and IFN-β expression were quantified by qRT-PCR. **c**, Empty virus like particles were produced in scramble-293T cells or siFTSJ3 and used to transduce U937 cells. IFN-α and IFN-β expression were quantified by qRT-PCR 16 hours later. **d**, RT-mutant HIV_{BaL} virus produced in scramble or siFTSJ3 cells was used to infect U937 cells.Type-1 interferons were quantified by qRT-PCR 16 h.p.i. FTSJ3 expression knockdown in HIV producing cells was assessed by western blot (left panel). n=3, results shown as the mean ±s.d.**p≤0.005 by two-tailed Student's *t*-test.

Extended Data Figure 7 : Characterization of shMDA5 and shRIG-I knock-down U937 cells.

a, Inhibition of RIG-I using shRNA in U937 assessed by western blot. **b**, U937-shMDA5 and U937-shRIG-I were characterized for their ability to induce IFN-β after polyI:C treatment or Sendai virus infection. **c**, Type-I interferons expression in U937 or U937-shRIG-I cells infected by siFTSJ3-HIV viral particles. IFN-α and IFN-β were quantified by qRT-PCR 16 h.p.i. n=3, results shown as the mean ±s.d.**p ≤ 0.05; *p≤0.01 by two-tailed Student's *t*-test.

Extended Data Figure 8: siFTSJ3-HIV induces phosphorylation of IRF-3, IRF-7 and Stat-1 transcriptional regulators and type-I interferons expression in monocyte-derived macrophages (MDM).

a, Monocytes were purified from human peripheral blood mononuclear cells from healthy donors using CD14 selection magnetic beads. Monocytes were differentiated using GM-CSF for 5 days into macrophages and checked by FACS analysis. Same amounts of wt-HIV or siFTSJ3-HIV were used to infect primary cells. 4 hours later, IRF3, IRF7 and Stat-1 phosphorylation was assessed by western blot. ERK-1/2 level was assessed as a loading control. **b**, 16 hours post-infection, cells were harvested and RNAs purified. IFN-α and IFN-β were quantified using qRT-PCR and normalized to actin. Results are expressed as fold increase compared to uninfected cells. n=3, results shown as the mean ±s.d. **$p \leq 0.05$;****$p \leq 0.0001$ by two-tailed Student's *t*-test.

Acknowledgements:

We thank Prof. Monsef Benkirane and members of the Molecular Virology laboratory for support and critical reading of the manuscript. This work was supported by grants from the European FP7 contract 201412, MSDAvenir, and FRM 'équipe labéllisée' to Monsef Benkirane, head of the molecular virology lab. This work was also supported by an ANR HTRNAMod (ANR-13-ISV8-0001) grant to Y.M. M.R. was supported by "Région Languedoc Roussillon".

Contributions

Y.B. conceived the study. Y.B. and M.R. designed experiments, interpreted data. V.M. and Y.M. realized RiboMethSeq experiments, analyzed and interpreted data. E.D. realized internal methylation assay experiments. Y.B. and M.R. wrote the paper. All the authors discussed the data, read and approved the final manuscript.

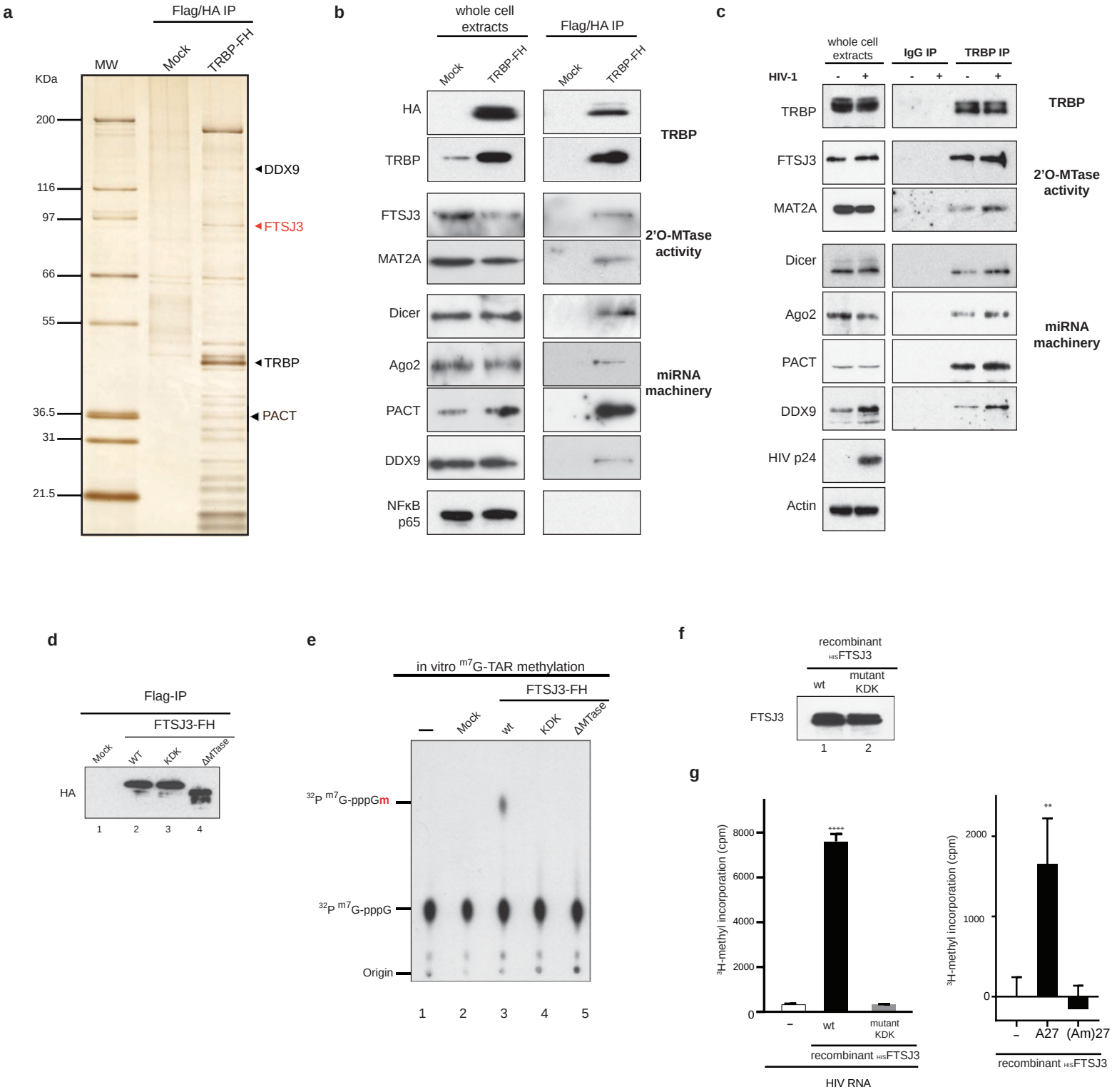
a
Flag/HA IP
MW
Mock
TRBP-FH
KDa
200
116
97
66
55
36.5
31
21.5
DDX9
FTSJ3
TRBP
PACT
b
whole cell extracts
Flag/HA IP
Mock
TRBP-FH
HA
TRBP
FTSJ3
MAT2A
Dicer
Ago2
PACT
DDX9
NFκB p65
TRBP
2'O-MTase activity
miRNA machinery
c
whole cell extracts
IgG IP
TRBP IP
HIV-1
TRBP
FTSJ3
MAT2A
Dicer
Ago2
PACT
DDX9
HIV p24
Actin
TRBP
2'O-MTase activity
miRNA machinery
d
Flag-IP
FTSJ3-FH
Mock
WT
KDK
ΔMTase
HA
1
2
3
4
e
in vitro m7G-TAR methylation
FTSJ3-FH
Mock
wt
KDK
ΔMTase
32P m7G-pppGm
32P m7G-pppG
Origin
1
2
3
4
5
f
recombinant HISFTSJ3
wt
mutant KDK
FTSJ3
1
2
g
3H-methyl incorporation (cpm)
8000
6000
4000
2000
0
****
–
wt
mutant KDK
recombinant HISFTSJ3
HIV RNA
2000
1000
0
**
–
A27
(Am)27
recombinant HISFTSJ3

Figure 1

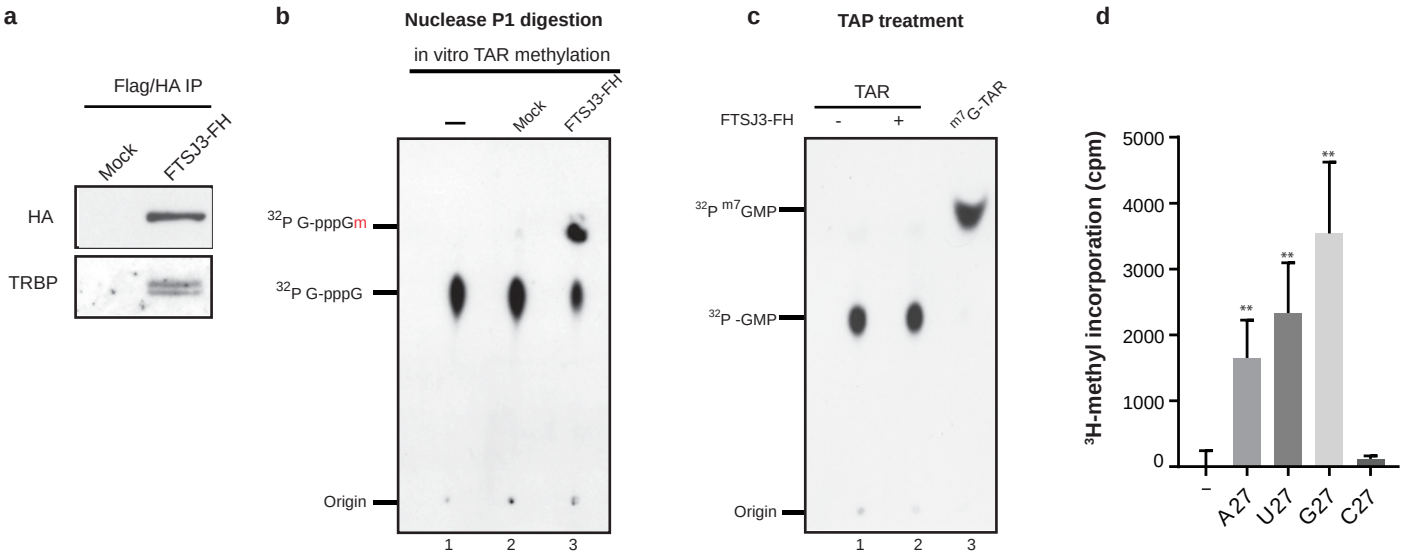

Extended Data Figure 1 | FTSJ3 is a 2'-O-methyltransferase. a, Reciprocal immunoprecipitation was realized on HeLa S3 cells expressing Flag/HA double tagged FTSJ3 protein (FTSJ3-FH). Eluates were analyzed using anti-HA and anti-TRBP antibodies. **b,** FTSJ3 methylation activity was assessed in vitro using TAR RNA as a substrate. Radiolabelled ^{32}P-TAR was incubated for 1 hour at 30°C with equal amounts of Flag/HA immunoprecipitated FSTJ3-FH or mock IP blotted in Fig 1d. RNA were then treated with nuclease P1 for 3 hours, and released caps were analysed by TLC chromatography migration using 0,3M ammonium sulfate buffer. Plate was dried and exposed by autoradiography. **c**, Products from in vitro mock and FTSJ3-FH TAR methylation were digested with tobacco acid pyrophosphatase (TAP). As a control, ^{32}P-^{m7}G-TAR was also digested with TAP, to release ^{m7}GMP residue. Products are analyzed on TLC plate developed with 0.45M ammonium sulfate buffer. **d**, Purified recombinant FTSJ3 was incubated without exogenous RNA (-) or with homopolymeric synthetic 27-mer RNAs A27, U27, G27 and C27 and associated MTase activity was determined by filter binding assay. The background obtained in absence of exogenous RNA was subtracted. N = 3, results shown as the mean ± s.d. **P ≤ 0.005 by two-tailed Student's t-test.

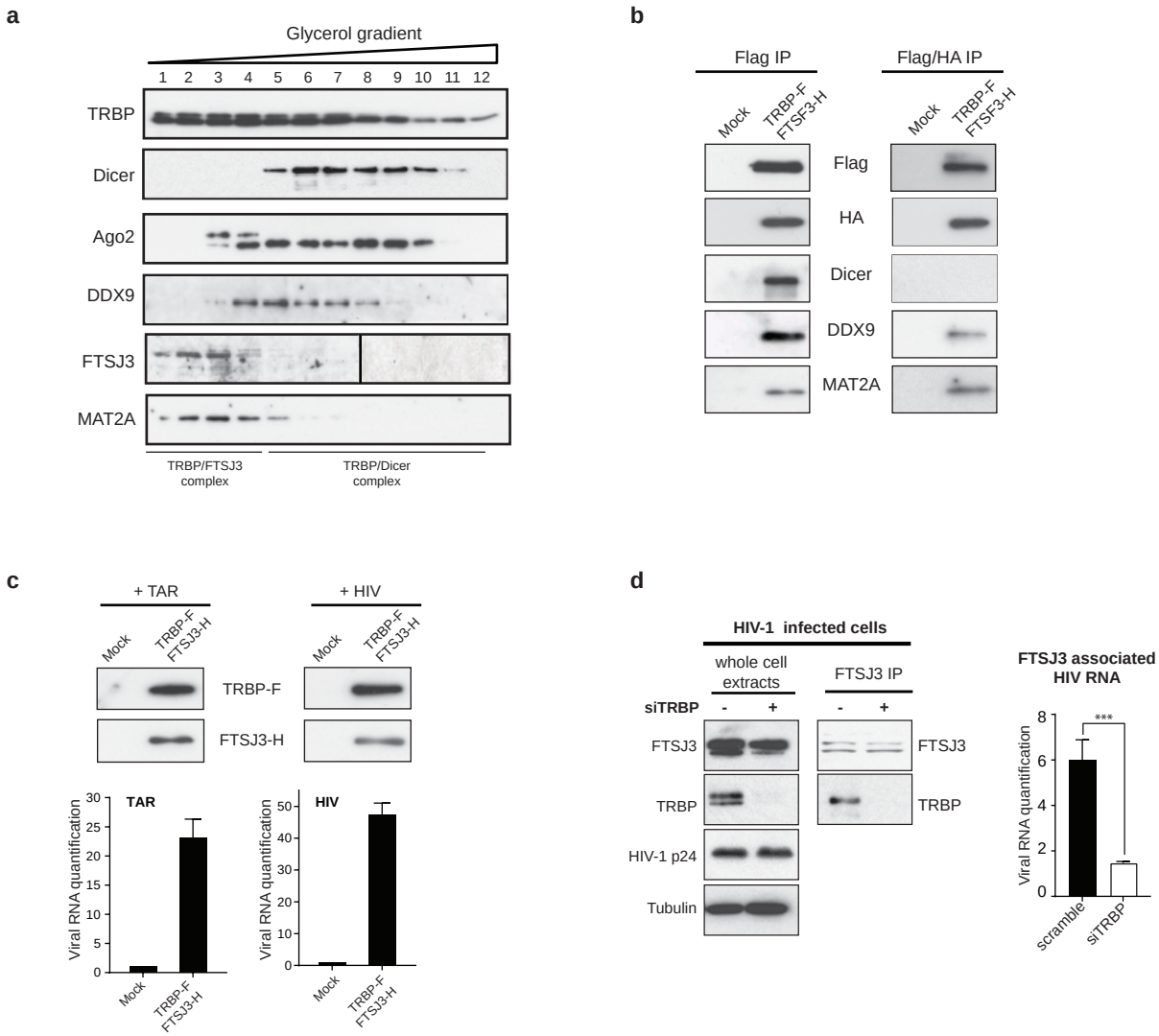
a
Glycerol gradient
1 2 3 4 5 6 7 8 9 10 11 12
TRBP
Dicer
Ago2
DDX9
FTSJ3
MAT2A
TRBP/FTSJ3 complex
TRBP/Dicer complex
b
Flag IP
Flag/HA IP
Mock
TRBP-F FTSF3-H
Flag
HA
Dicer
DDX9
MAT2A
c
+ TAR
+ HIV
Mock
TRBP-F FTSJ3-H
TRBP-F
FTSJ3-H
TAR
HIV
Viral RNA quantification
d
HIV-1 infected cells
whole cell extracts
FTSJ3 IP
siTRBP
FTSJ3
TRBP
HIV-1 p24
Tubulin
FTSJ3 associated HIV RNA
***
scramble
siTRBP

Figure 2

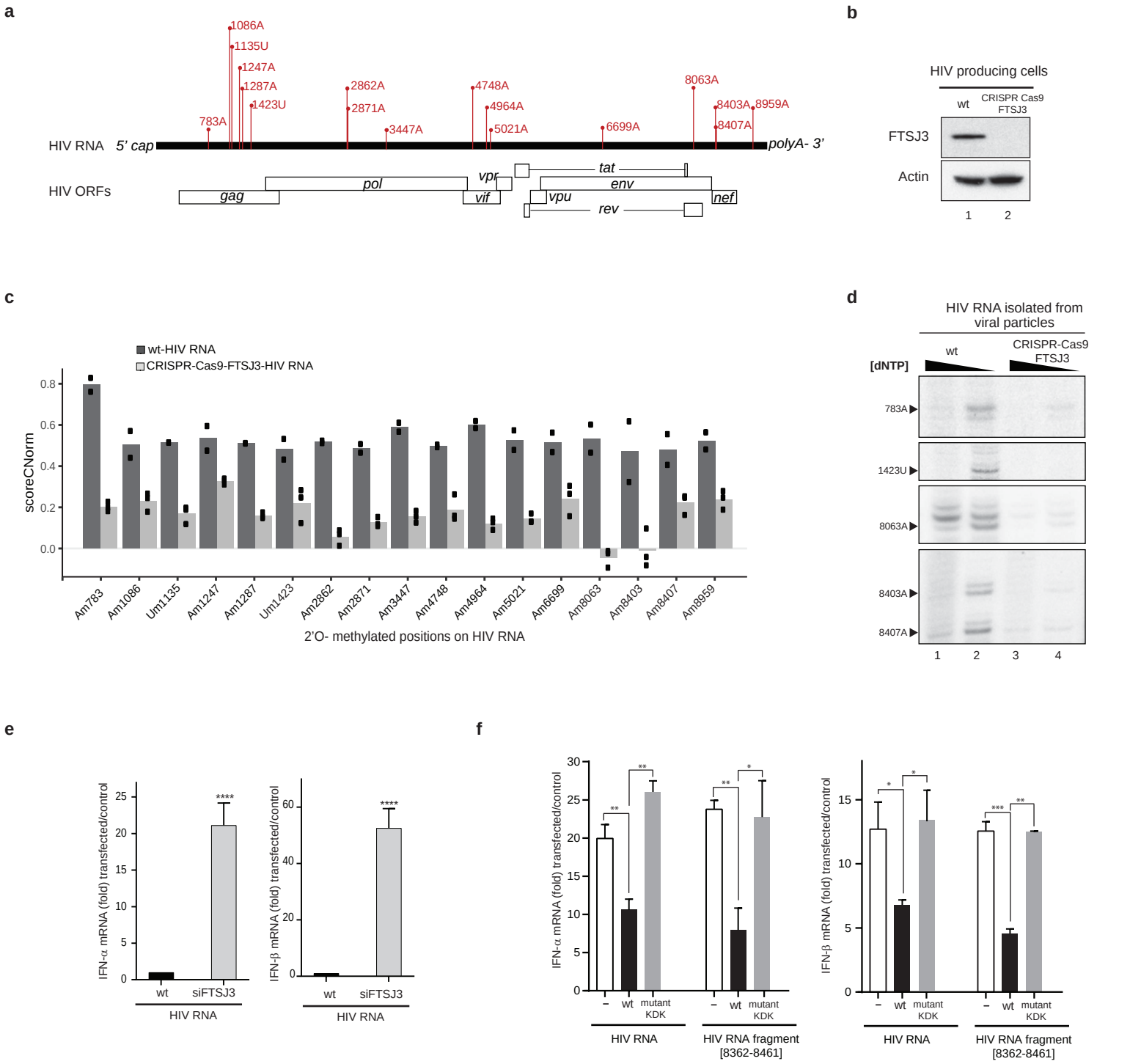
a
1086A
1135U
1247A
1287A
1423U
783A
2862A
2871A
3447A
4748A
4964A
5021A
6699A
8063A
8403A
8959A
8407A
HIV RNA
5' cap
polyA- 3'
HIV ORFs
gag
pol
vif
vpr
tat
env
vpu
rev
nef
b
HIV producing cells
wt
CRISPR Cas9 FTSJ3
FTSJ3
Actin
1
2
c
wt-HIV RNA
CRISPR-Cas9-FTSJ3-HIV RNA
scoreCNorm
0.0
0.2
0.4
0.6
0.8
Am783
Am1086
Um1135
Am1247
Am1287
Um1423
Am2862
Am2871
Am3447
Am4748
Am4964
Am5021
Am6699
Am8063
Am8403
Am8407
Am8959
2'O- methylated positions on HIV RNA
d
HIV RNA isolated from viral particles
wt
CRISPR-Cas9 FTSJ3
[dNTP]
783A
1423U
8063A
8403A
8407A
1
2
3
4
e
IFN-α mRNA (fold) transfected/control
IFN-β mRNA (fold) transfected/control
wt
siFTSJ3
HIV RNA
f
IFN-α mRNA (fold) transfected/control
IFN-β mRNA (fold) transfected/control
–
wt
mutant KDK
HIV RNA
HIV RNA fragment [8362-8461]

Figure 3

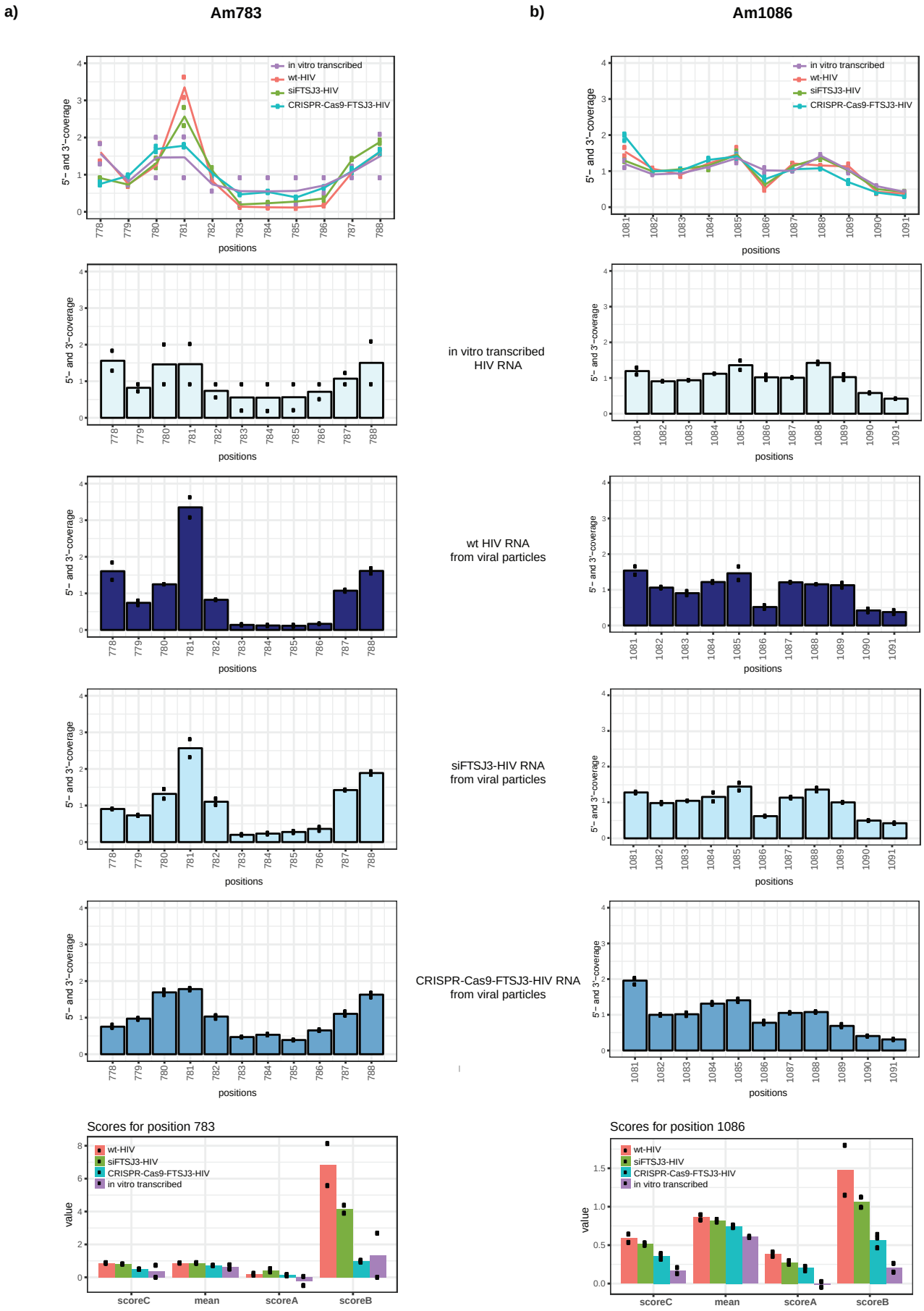

Extended Data Figure 2 | RiboMethSeq analysis of 2'-O-methylated sites detected in HIV RNA isolated from viral particles: **a-q**, For each of the seventeen 2'-O-methylated sites, RiboMethSeq data are presented from top to bottom: Top panel:Superposed relative local cleavage profiles for four conditions (transcript, wt-HIV-1 RNA, siFTSJ3-HIV-1 RNA and CRISPR-Cas9-FTSJ3-HIV-1 RNA). Middle panel:Relative local cleavage profile for in vitro T7 transcript of HIV-1 RNA, for wt-HIV-1 RNA, siFTSJ3-HIV-1 RNA and CRISPR-Cas9-FTSJ3-HIV-1 RNA extracted from virions. Error bars correspond to biological replicates, position numbers are indicated on the bottom. Lower panel: Variations and absolute values of RiboMethSeq scores (ScoreC, ScoreMean, Score A and Score B) for methylated position. ScoreC, ScoreMean and Score A generally vary from 0 to 1 (negative values are possible), while Score B may be > 1 for highly methylated positions in RNA. In RiboMethSeq the protection caused by 2'-O-methylation appears at the 3'-neighboring position in RNA. For simplicity -1 shift was applied to numbering here, thus increased protection signal falls exactly to 2'-O-methylated nucleotide. Error bars correspond to biological replicates; N=2, results shown as the mean ± s.d.

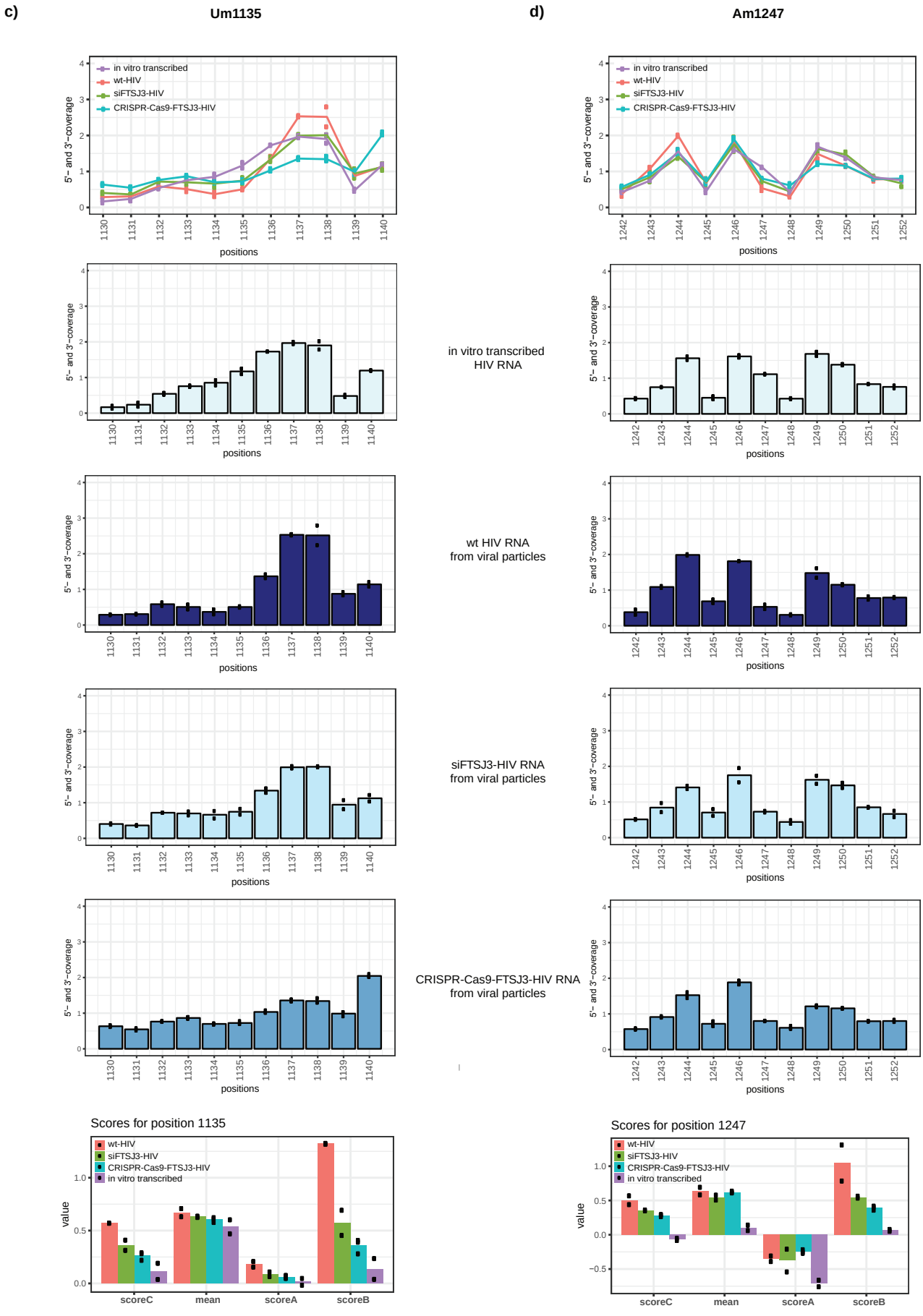

Extended Data Figure 2 | RiboMethSeq analysis of 2'-O methylated sites detected in HIV RNA isolated from viral particles (continued c, d)

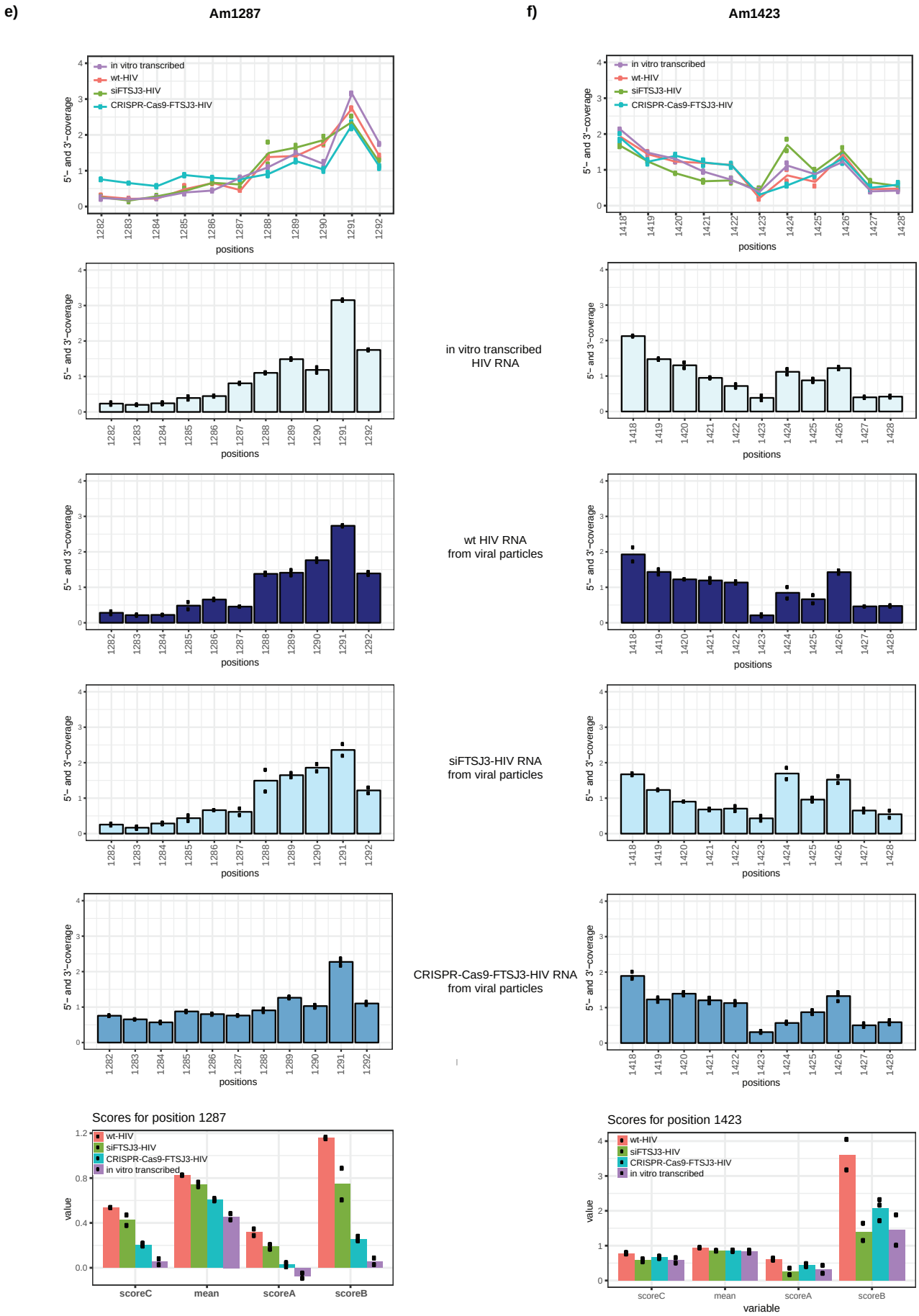

Extended Data Figure 2 | RiboMethSeq analysis of 2'-O methylated sites detected in HIV RNA isolated from viral particles (continued e, f)

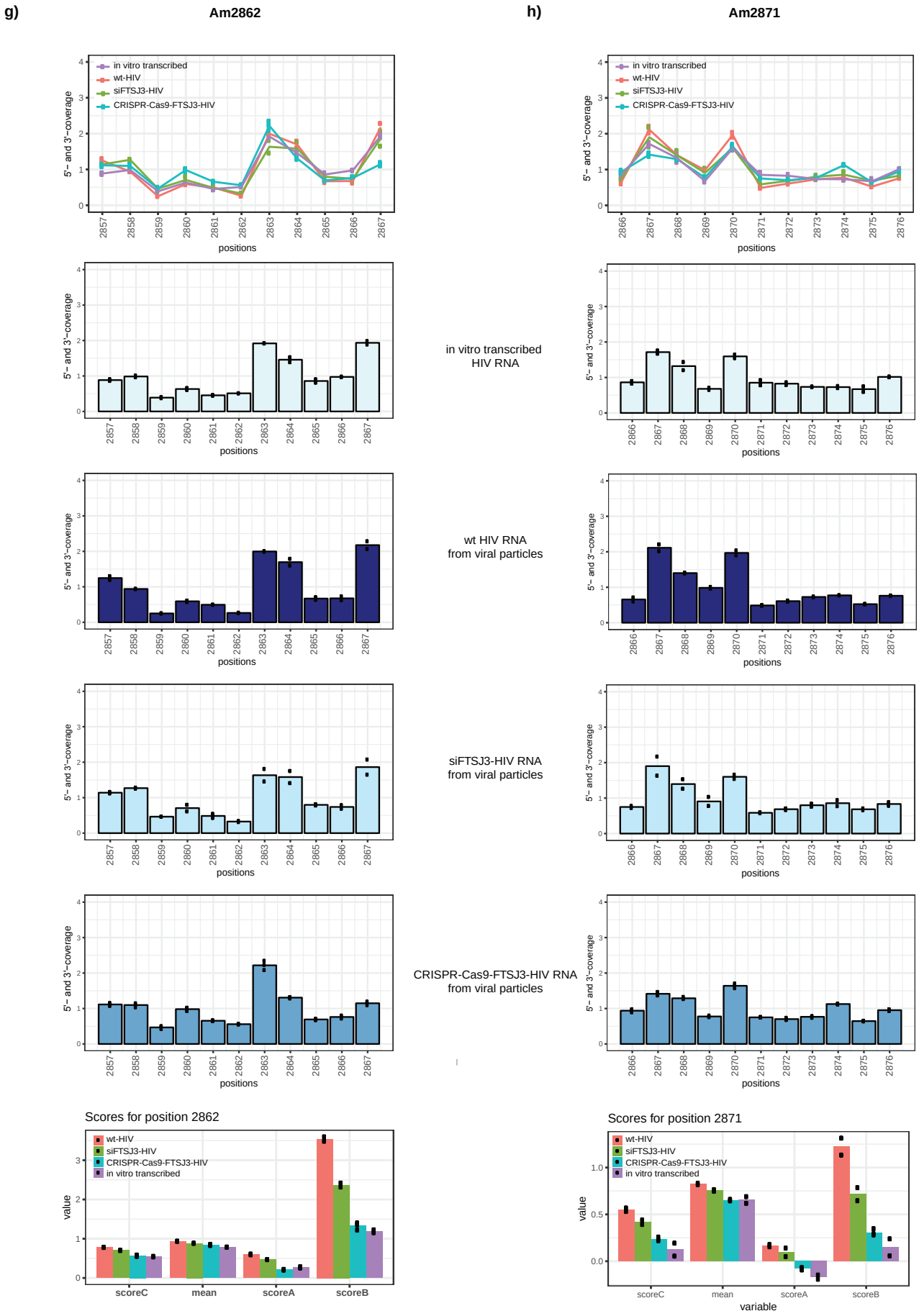

Extended Data Figure 2 | RiboMethSeq analysis of 2'-O methylated sites detected in HIV RNA isolated from viral particles (continued g, h)

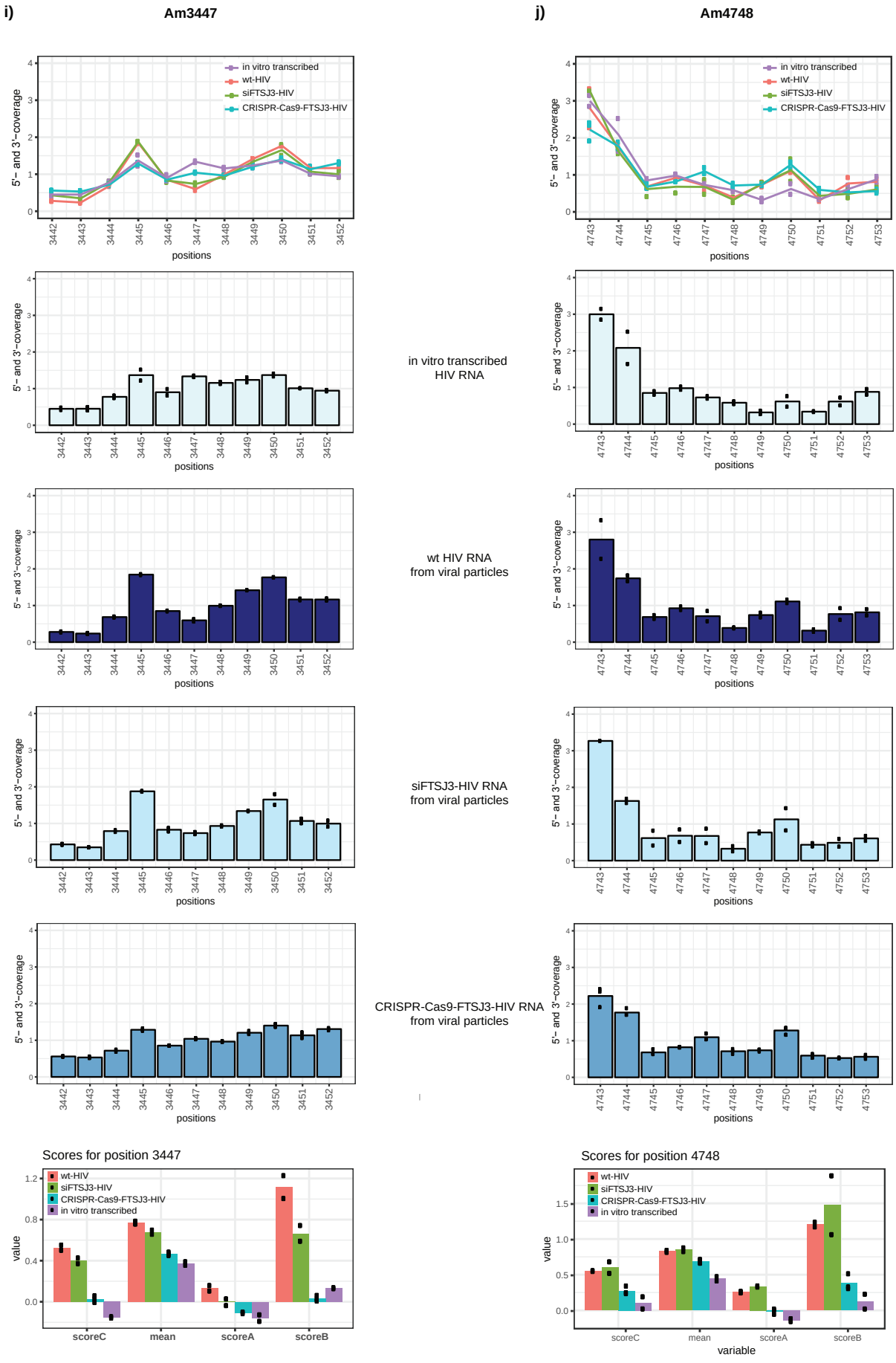

Extended Data Figure 2 | RiboMethSeq analysis of 2'-O methylated sites detected in HIV RNA isolated from viral particles (continued i, j)

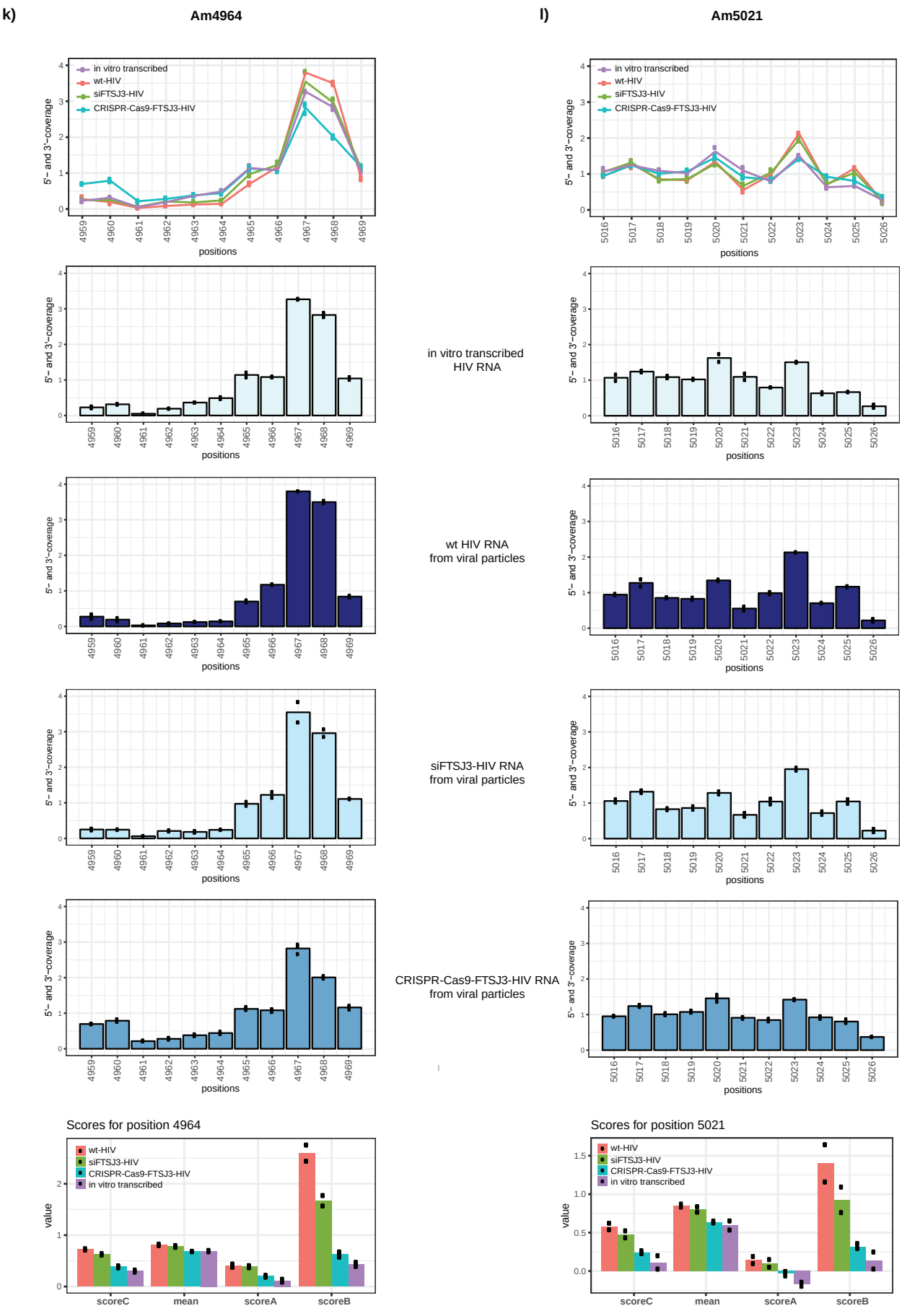

Extended Data Figure 2 | RiboMethSeq analysis of 2'-O methylated sites detected in HIV RNA isolated from viral particles (continued k, l)

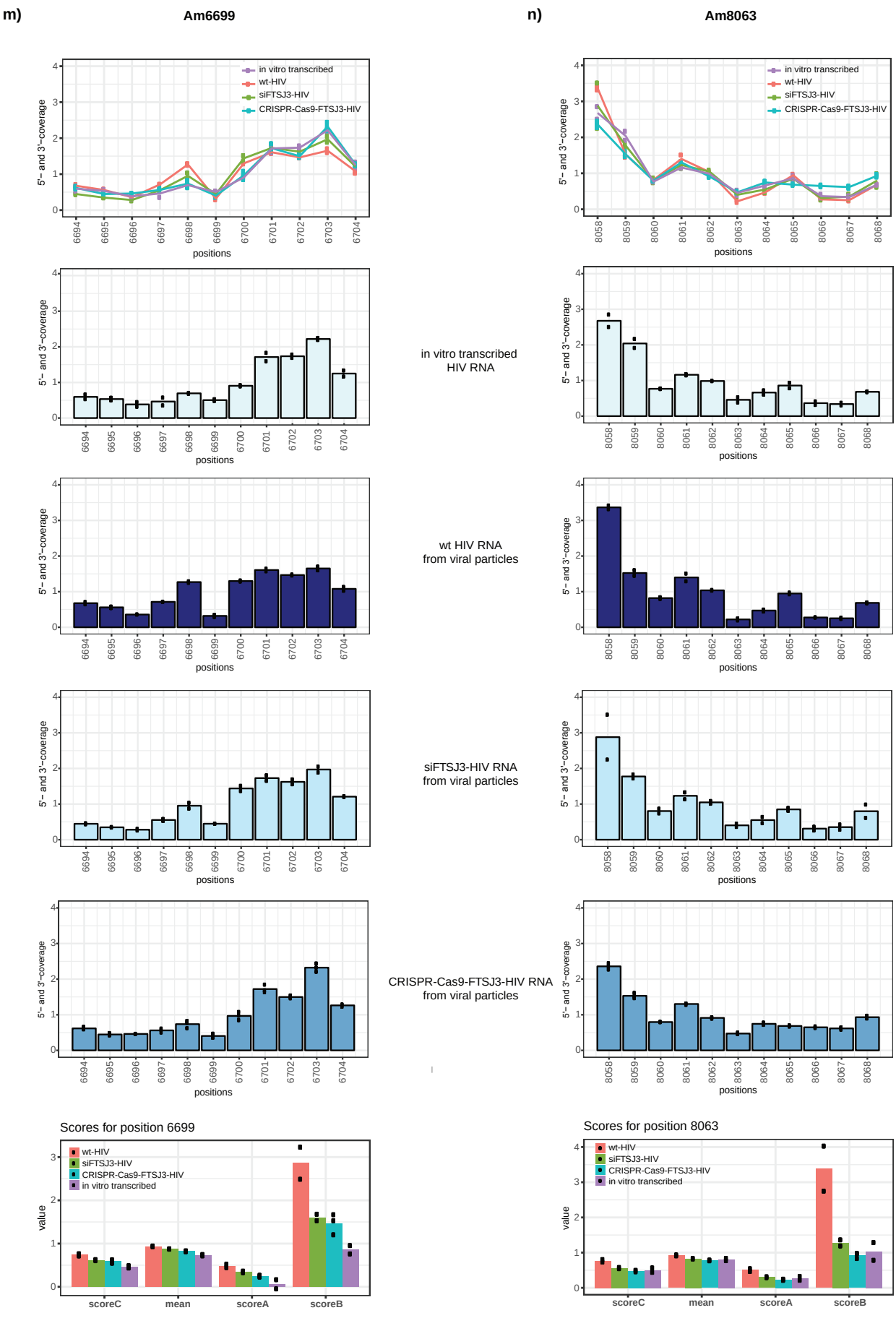

Extended Data Figure 2 | RiboMethSeq analysis of 2'-O methylated sites detected in HIV RNA isolated from viral particles (continued m, n)

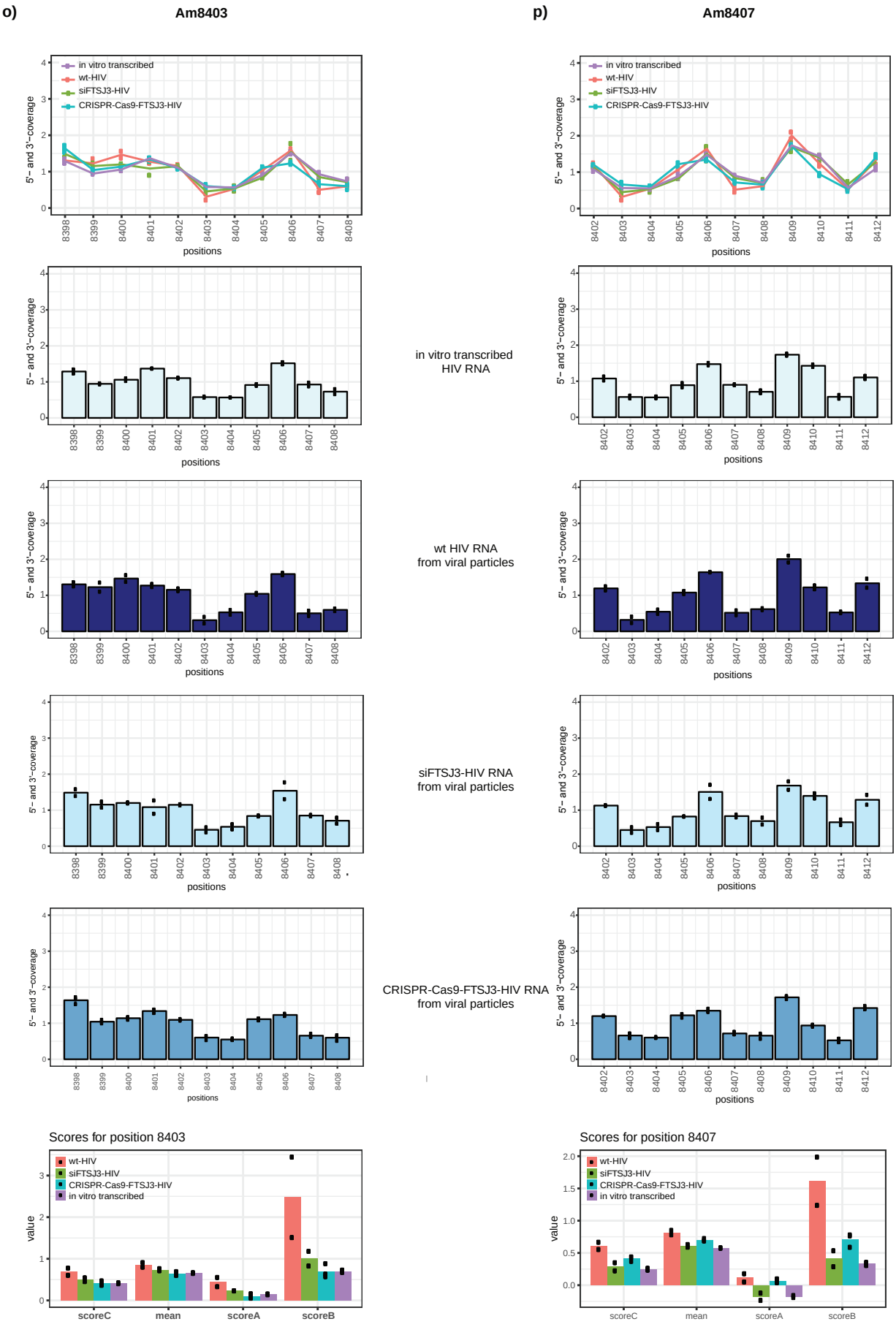

Extended Data Figure 2 | RiboMethSeq analysis of 2'-O methylated sites detected in HIV RNA isolated from viral particles (continued o, p)

q) **Am8959**

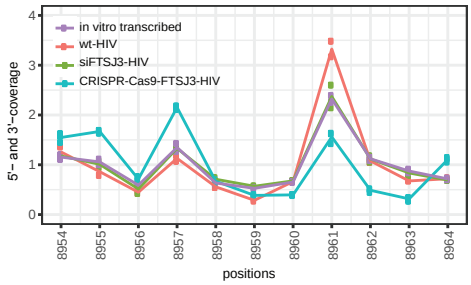

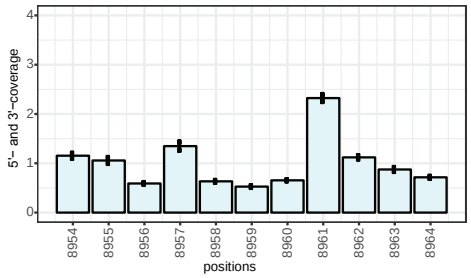

in vitro transcribed HIV RNA

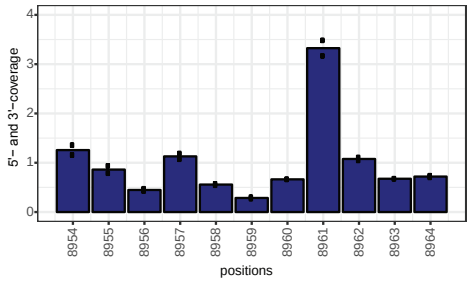

wt HIV RNA from viral particles

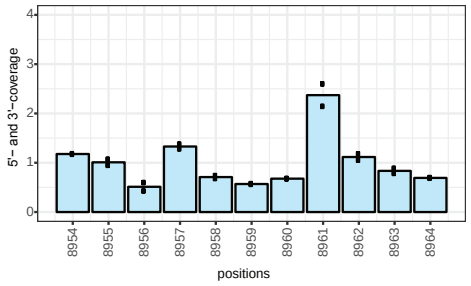

siFTSJ3-HIV RNA from viral particles

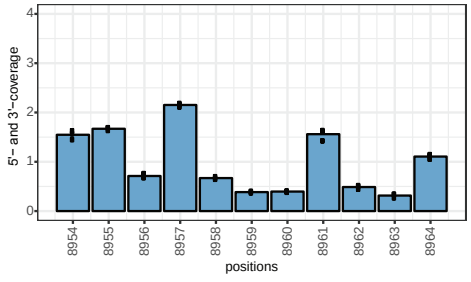

CRISPR-Cas9-FTSJ3-HIV RNA from viral particles

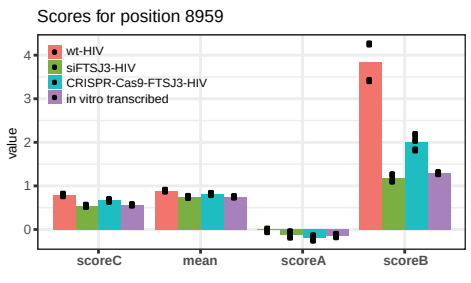

Extended Data Figure 2 | RiboMethSeq analysis of 2'-O methylated sites detected in HIV RNA isolated from viral particles (continued q)

Position	Residu	Conservation frequency (%)	number of non-gap sequences analysed	Residu frequency in major HIV-1 subtypes and circulating recombinant forms									
				B	A1	A2	C	D	F1	F2	G	CRF01_AE	CRF 02_AG
786	**A**	**99,84**	2435	1041/1044	168/168	3/3	676/676	65/65	31/31	8/8	66/66	272/272	101/101
1086	**A**	**99,63**	2436	1044/1045	168/168	3/3	670/676	65/65	31/31	8/8	65/67	272/272	101/101
1135	**U**	**99,84**	2436	1043/1045	168/168	3/3	674/676	65/65	31/31	8/8	67/67	272/272	101/101
1247	**A**	**74,92**	2436	1003/1045	0/168	1/3	665/676	64/65	31/31	8/8	36/67	0/272	17/101
1287	**A**	**99,79**	2436	1045/1045	168/168	3/3	671/676	65/65	31/31	8/8	67/67	272/272	101/101
1423	**U**	**99,96**	2436	1045/1045	168/168	3/3	675/676	65/65	31/31	8/8	67/67	272/272	101/101
2862	**A**	**99,92**	2436	1045/1045	168/168	3/3	675/676	64/65	31/31	8/8	67/67	272/272	101/101
2871	**A**	**99,79**	2435	1044/1044	168/168	3/3	673/676	64/65	31/31	8/8	67/67	271/272	101/101
3447	**A**	**96,67**	2434	982/1043	166/168	3/3	664/676	63/65	30/31	8/8	65/67	271/272	101/101
4748	**A**	**97,50**	2436	1019/1045	167/168	3/3	656/676	63/65	31/31	8/8	64/67	265/272	99/101
4964	**A**	**98,11**	2435	1025/1044	153/168	3/3	669/676	63/65	30/31	8/8	66/67	271/272	101/101
5021	**A**	**94,29**	2433	998/1043	145/168	0/3	626/676	63/65	30/31	8/8	63/67	267/271	94/101
6699	**A**	**92,69**	2434	915/1045	167/167	3/3	662/675	65/65	31/31	8/8	34/67	271/272	100/101
8063	**A**	**99,38**	2435	1037/1044	167/168	3/3	671/676	65/65	30/31	8/8	67/67	272/272	100/101
8403	**A**	**66,03**	2361	927/1000	5/162	0/3	534/664	53/65	1/30	2/6	8/60	8/272	21/99
8407	**A**	**96,47**	2407	988/1041	161/164	3/3	653/671	63/65	27/31	6/6	59/63	271/272	91/100
8959	**A**	**75,33**	1439	635/762	139/145	3/3	1/107	47/56	12/25	4/5	16/63	178/207	49/66

Extended Data Figure 3 | Conservation frequency of the seventeen identified 2'O-methylated residus among major HIV-1 subtypes and circulating recombinant forms. The 17 sites of 2'O-methylation identified on HIV-1 molecular clone, pNL4-3, were aligned to up to 2436 sequences of major HIV-1 subtypes and circulating recombinant forms sequences available on Los Alamos HIV database (http://www.hiv.lanl.gov/). The number of sequences analyzed for each position and the conservation frequency are presented in the table.

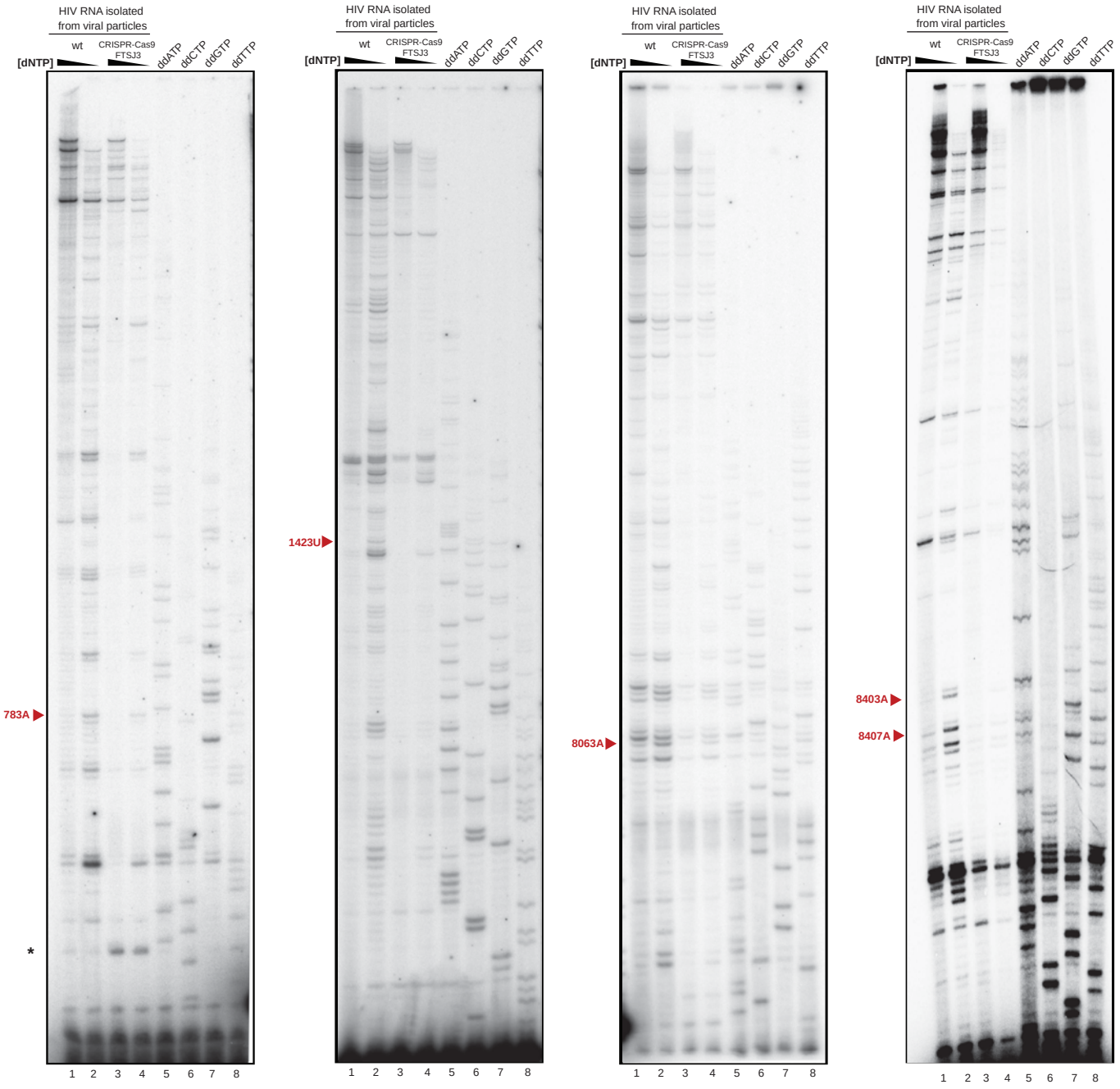

Extended Data Figure 4 | Validation of 783A, 1423U, 8063A, 8403A and 8407A 2'-O-methylations using primer extension assay. HIV-1 RNA isolated from viral particles produced in mock cells (wt) or cells knocked-out for FTSJ3 using CRISPR-Cas9 (CRISPR-Cas9-FTSJ3) were subjected to primer extension assay using specific radiolabelled primers. Extension assay was realized in high (1,3) and low concentrations (2,4) of dNTP as indicated. Sequencing experiment was run side by side using wt-HIV RNA as a template (4-8). Primer extension products were analyzed on acrylamide-urea sequencing gel and visualized by autoradiography. 2'O-methylated position and stop is indicated by an arrow.

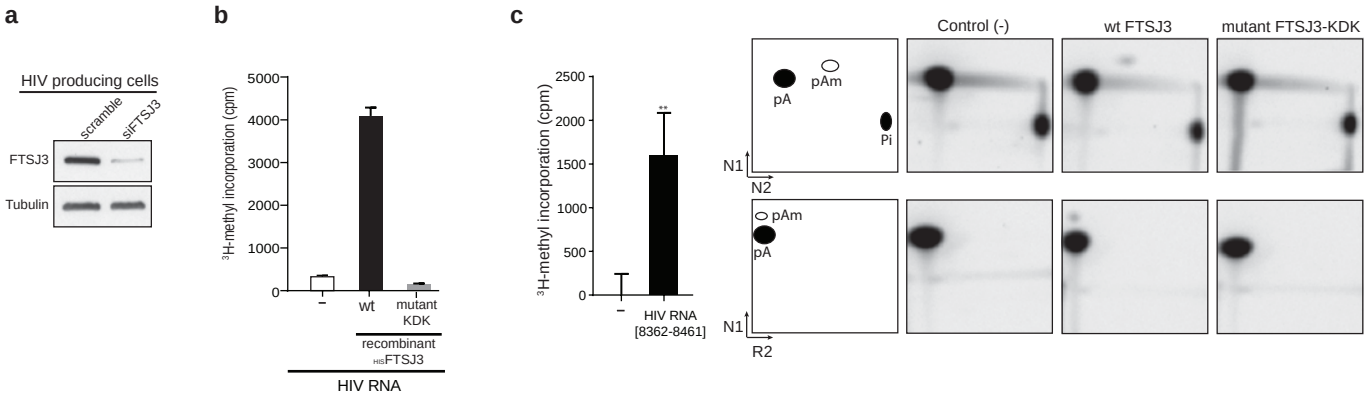

Extended Data Figure 5 | Characterization of HIV-1 RNA transfected in U937 cells. **a**, HIV viruses were produced in 293T cells transfected with FTSJ3 siRNA or a control non specific siRNA (scramble). FTSJ3 inhibition was assessed by western blot. **b**, Purified recombinant $_{HIS}$FTSJ3 wt or catalytic mutant KDKE was incubated with in vitro transcribed HIV-1 RNA in presence of radiolabeled ^{3}H-SAM and MTase activity was determined by filter binding assay (FBA) **c**, Purified recombinant wt-FTSJ3 was incubated without exogenous RNA or with the [8362-8461] HIV RNA fragment and MTase activity was determined by FBA (left panel) or 2D TLC separation (right panel). FBA results were normalized by substracting the background obtained in absence of exogenous RNA. 2D TLC separation of 5'-[^{32}P-NMP] resulted from nuclease P1 hydrolysis of HIV RNA transcript [8362-8461] radiolabeled with [α-^{32}P]ATP and incubated with wt-FTSJ3 or mutant KDKE- FTSJ3 recombinant proteins. Migration was performed in N1/N2 or N1/R2 combination of solvents as described in Methods section. Positions of unmodified AMP (pA) and 2'-O-methyl AMP (pAm), inorganic phosphate (Pi) are indicated.

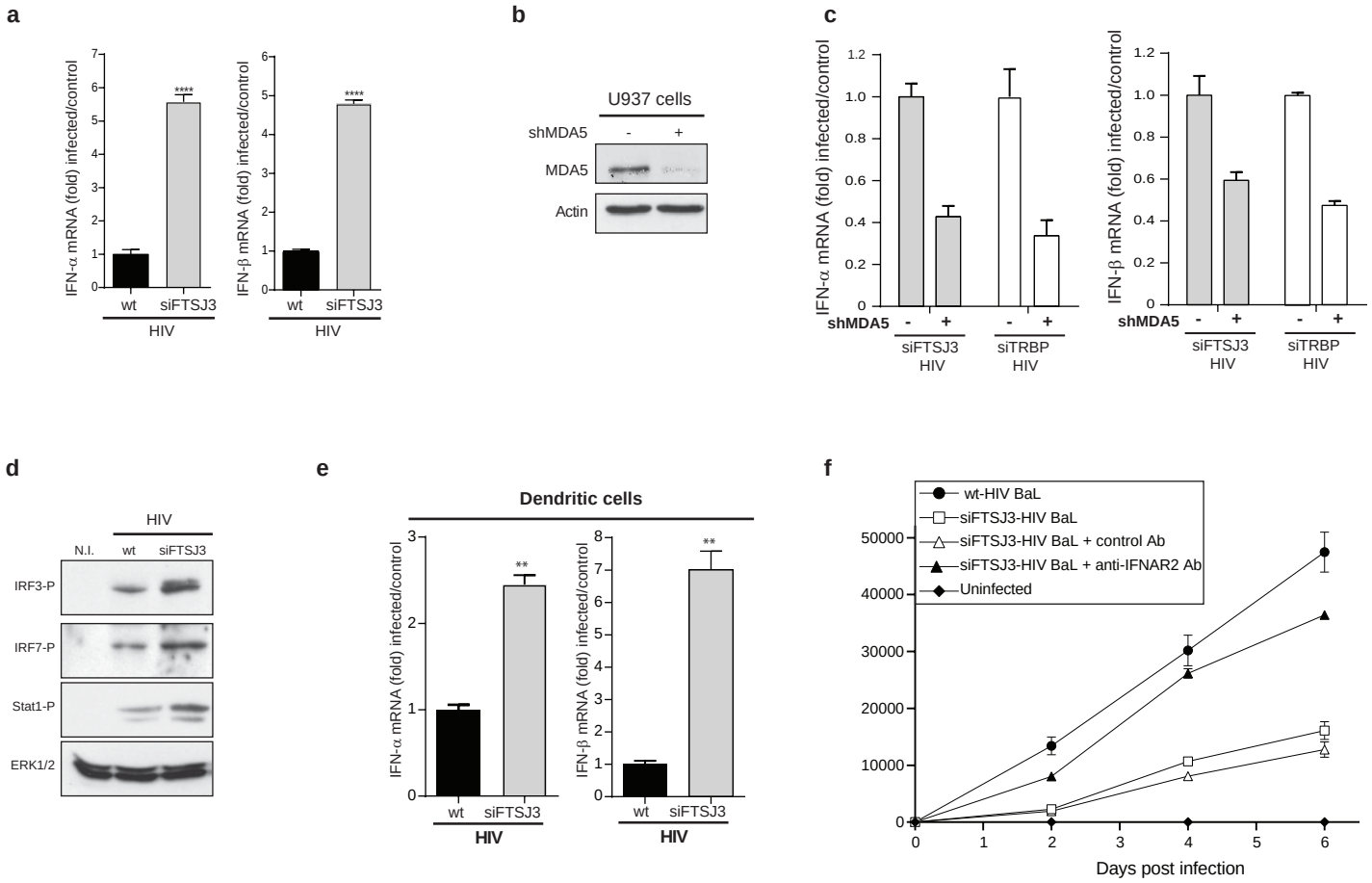
a
IFN-α mRNA (fold) infected/control
IFN-β mRNA (fold) infected/control
****
wt
siFTSJ3
HIV
b
U937 cells
shMDA5
MDA5
Actin
c
IFN-α mRNA (fold) infected/control
IFN-β mRNA (fold) infected/control
shMDA5
siFTSJ3
siTRBP
HIV
d
HIV
N.I.
wt
siFTSJ3
IRF3-P
IRF7-P
Stat1-P
ERK1/2
e
Dendritic cells
IFN-α mRNA (fold) infected/control
IFN-β mRNA (fold) infected/control
**
f
wt-HIV BaL
siFTSJ3-HIV BaL
siFTSJ3-HIV BaL + control Ab
siFTSJ3-HIV BaL + anti-IFNAR2 Ab
Uninfected
Days post infection

Figure 4

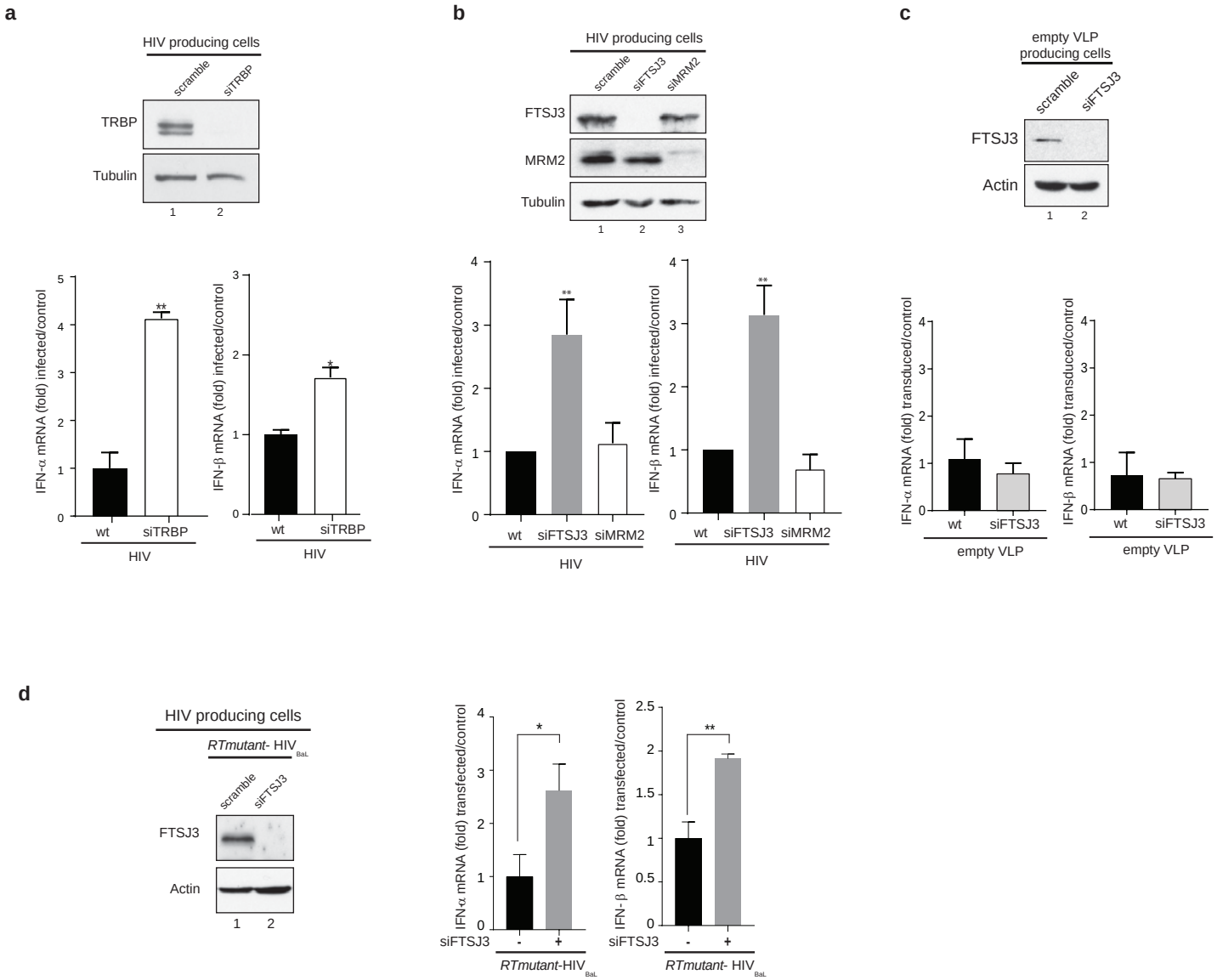

Extended Data Figure 6 | HIV viral particles produced in TRBP knock-down cells induce type-I interferons expression while viruses produced in siMRM2 knocked-down, and siFTSJ3-emply virus-like particles do not. **a**, 293T cells were transfected with siRNA targeting TRBP (siTRBP) (in **a**), FTSJ3 (siFTSJ3) or MRM2 (siMRM2) (in **b**) or a control non-specific siRNA (scramble). 16 hours post-transfection, cells were further transfected with pNL4-3 HIV molecular clone. Viruses were harvested 48 hours later and quantified for RT, p24 and packaged viral RNA. Protein inhibition was assessed by western blot (upper panels). U937 cells were infected with same amounts of viruses produced in cells treated with scramble siRNA (wt-HIV) or siTRBP, siFTSJ3, siMRM2 as indicated. 16 hours later, IFN-α and IFN-β expression were quantified by qRT-PCR. **c**, Empty virus like particles were produced in scramble-293T cells or siFTSJ3 and used to transduce U937 cells. IFN-α and IFN-β expression were quantified by qRT-PCR 16 hours later. **d**, RT-mutant HIV_{BaL} virus produced in scramble or siFTSJ3 cells was used to infect U937 cells.Type-1 interferons were quantified by qRT-PCR 16 h.p.i. FTSJ3 expression knockdown in HIV producing cells was assessed by western blot (left panel). N=3, results shown as the mean ±s.d.**P≤0.005 by two-tailed Student's t-test.

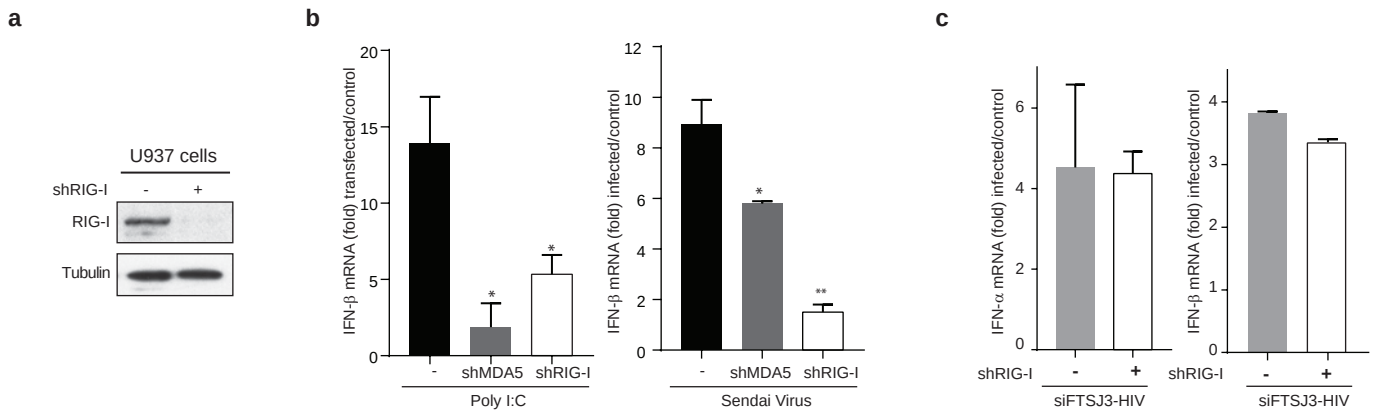

Extended Data Figure 7 | Characterization of shMDA5 and shRIG-I knock-down U937 cells. a, Inhibition of RIG-I using shRNA in U937 assessed by western blot. **b**, U937-shMDA5 and U937-shRIG-I were characterized for their ability to induce IFN-β after polyI:C treatment (500ng/ml) or Sendai virus infection (10^5 $CEID_{50}$/ml). **c**, Type-I interferons expression in U937 or U937-shRIG-I cells infected by siFTSJ3-HIV viral particles. IFN-α and IFN-β were quantified by qRT-PCR 16 h.p.i. N=3, results shown as the mean±s.d.**P≤0.05; *P≤0.01 by two-tailed Student's t-test.

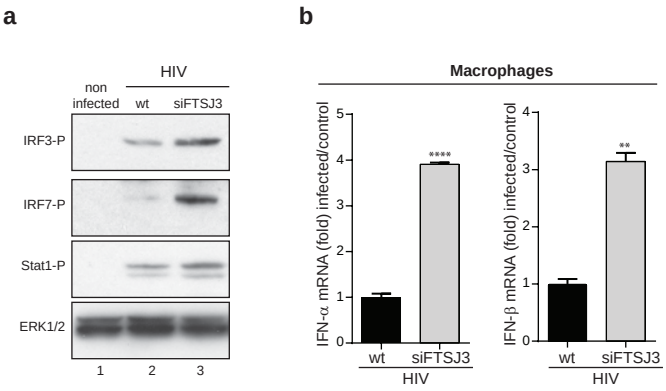

Extended Data Figure 8 | siFTSJ3-HIV induces phosphorylation of IRF3, IRF7 and Stat-1 transcriptional regulators and type-I interferons expression in monocyte-derived macrocophages (MDM). a, Monocytes were purified from human peripheral blood mononuclear cells from healthy donors using CD14 selection magnetic beads. Monocytes were differentiated using GM-CSF for 5 days into macrophages and checked by FACS analysis. Same amounts of wt-HIV or siFTSJ3-HIV were used to infect primary cells. 4 hours later, IRF3, IRF7 and Stat-1 phosphorylation was assessed by western blot. ERK-1/2 level was assessed as a loading control. **b**, 16 hours post-infection, cells were harvested and RNAs purified. IFN-α and IFN-β were quantified using qRT-PCR and normalized to actin. Results are expressed as fold increase compared to uninfected cells. N=3, results shown as the mean ±s.d.**P≤0.05;****P≤0.0001 by two-tailed Student's t-test.